Wino dark matter searches with dwarf spheroidal galaxies

Koji Ishiwata

Kanazawa University

PRD 104, no.2, 023016 (with S. Ando)

SUSY2021, China, August 23, 2021

Plan to talk

1. Introduction
2. Indirect searches with dwarf spheroidal galaxies
3. Numerical results
4. Conclusions

1. Introduction

Evidences for dark matter

- Rotation curve of galaxies
- Bullet clusters
- Cosmic microwave background (CMB)

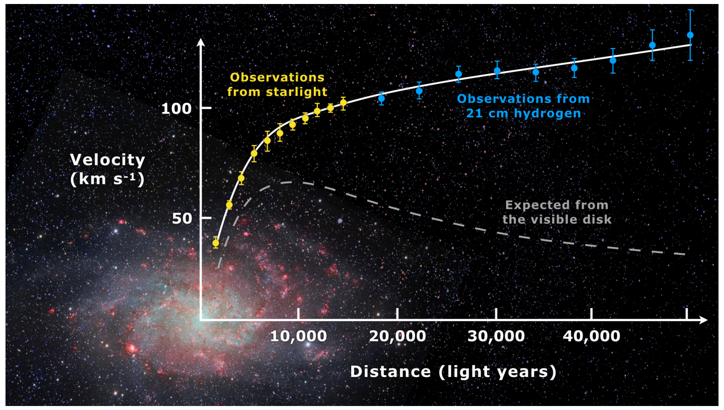

Corbelli, Salucci ’00

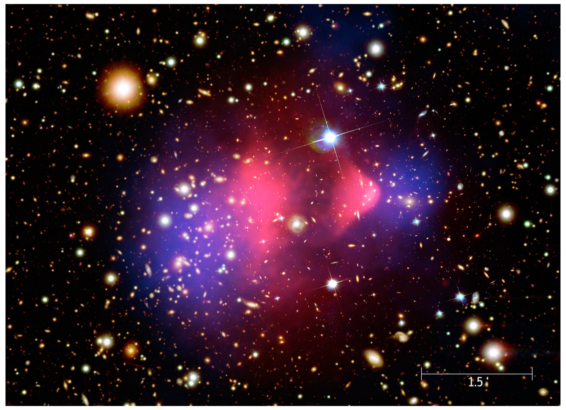

Markevitch et al. ’04
Clowe et al. ’04

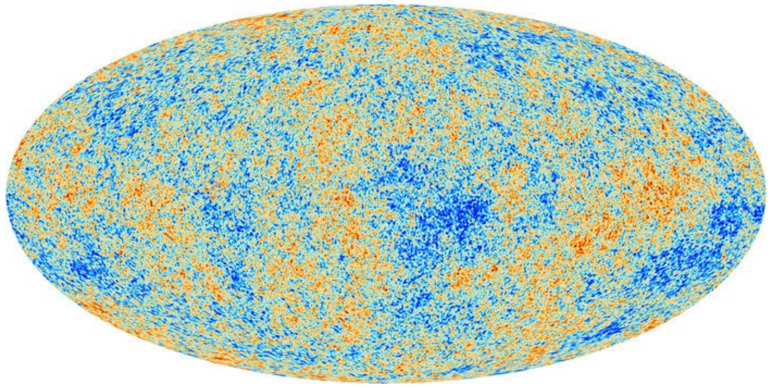

Planck ’13

Evidences for dark matter

- Rotation curve of galaxies
- Bullet clusters
- Cosmic microwave background (CMB)

However, there’s no candidate for DM in the standard model (SM) of particle physics

Corbelli, Salucci ’00

Markevitch et al. ’04
Clowe et al. ’04

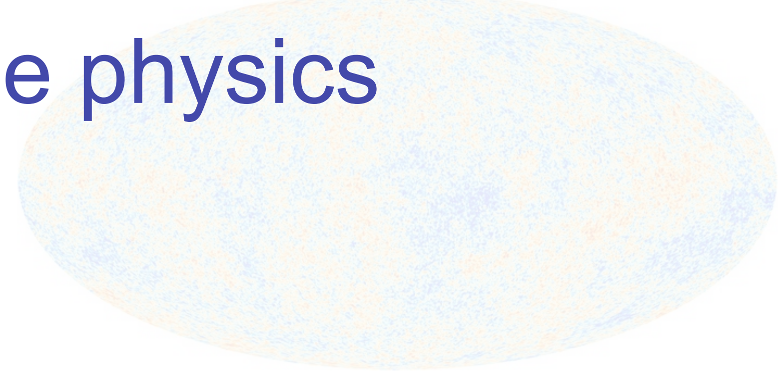

Planck ’13

→ Beyond the SM is needed

(DM is a key to find the new physics)

To be consistent the observations, DM has to be

- Electrically neutral
- Non-baryonic
- Stable or sufficiently long-lived
- Its energy density should agree with the CMB observations
- Non-relativistic

To be consistent the observations, DM has to be

- Electrically neutral
- Non-baryonic
- Stable or sufficiently long-lived
- Its energy density should agree with the CMB observations
- Non-relativistic

→ Weakly interacting massive particles (WIMPs) are good candidates

Features of the WIMP DM scenario

- DM abundance is naturally explained

- Promising theoretical models

  e.g.,

  Minimal supersymmetric extension of the SM (MSSM)

- It can be probed in direct/indirect detection experiments

Features of the WIMP DM scenario

- DM abundance is naturally explained

- Promising theoretical models

  e.g.,

  ★ Minimal supersymmetric extension of the SM (MSSM)

- It can be probed in direct/indirect detection experiments

After the discovery of

- 125 GeV Higgs
- No other new particles

The simplest interpretation would be

High-scale supersymmetry

e.g.,

Wells ’03

Giudice et al. ’04, ’12

Arkani-Hamed et al. ’05, ’05

Hall et al. ’10, ’12

High-scale supersymmetry

- Wino and higgsino are around TeV scale
- The other superparticles are much heavier

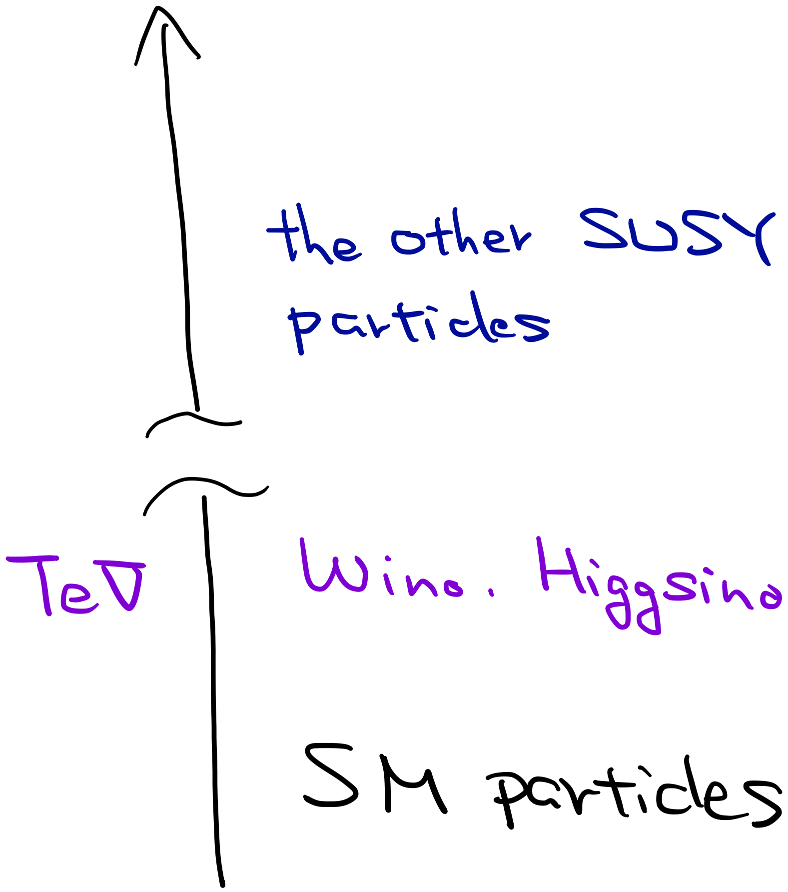

High-scale supersymmetry

- Wino and higgsino are around TeV scale
- The other superparticles are much heavier

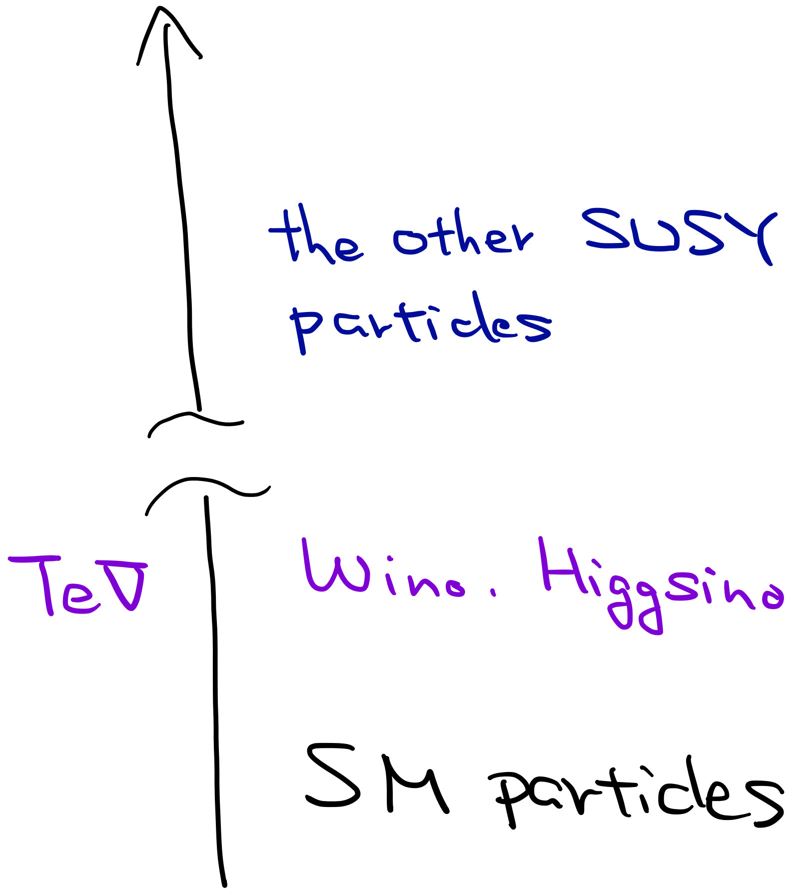

→ SM + Wino and Higgsino (up to TeV scale)

DM candidates

	$\mathrm{SU}(2)_L$	$\mathrm{U}(1)_Y$
● Wino	$\mathbf{3}$	0
● Higgsino	$\mathbf{2}$	$1/2$

“ElectroWeakly Interacting Massive Particles”

	$\mathrm{SU}(2)_L$	$\mathrm{U}(1)_Y$
★ ● Wino	$\mathbf{3}$	0
● Higgsino	$\mathbf{2}$	$1/2$

“ElectroWeakly Interacting Massive Particles”

Features of the WIMP DM scenario

- DM abundance is naturally explained

- Promising theoretical models

  e.g.,

  Minimal supersymmetric extension of the SM (MSSM)

- It can be probed in direct/indirect detection experiments

Features of the WIMP DM scenario

- DM abundance is naturally explained

- Promising theoretical models

  e.g.,

  Minimal supersymmetric extension of the SM (MSSM)

- It can be probed in **direct**/indirect detection experiments

Direct detection of Wino DM

Hisano, KI, Nagata '15

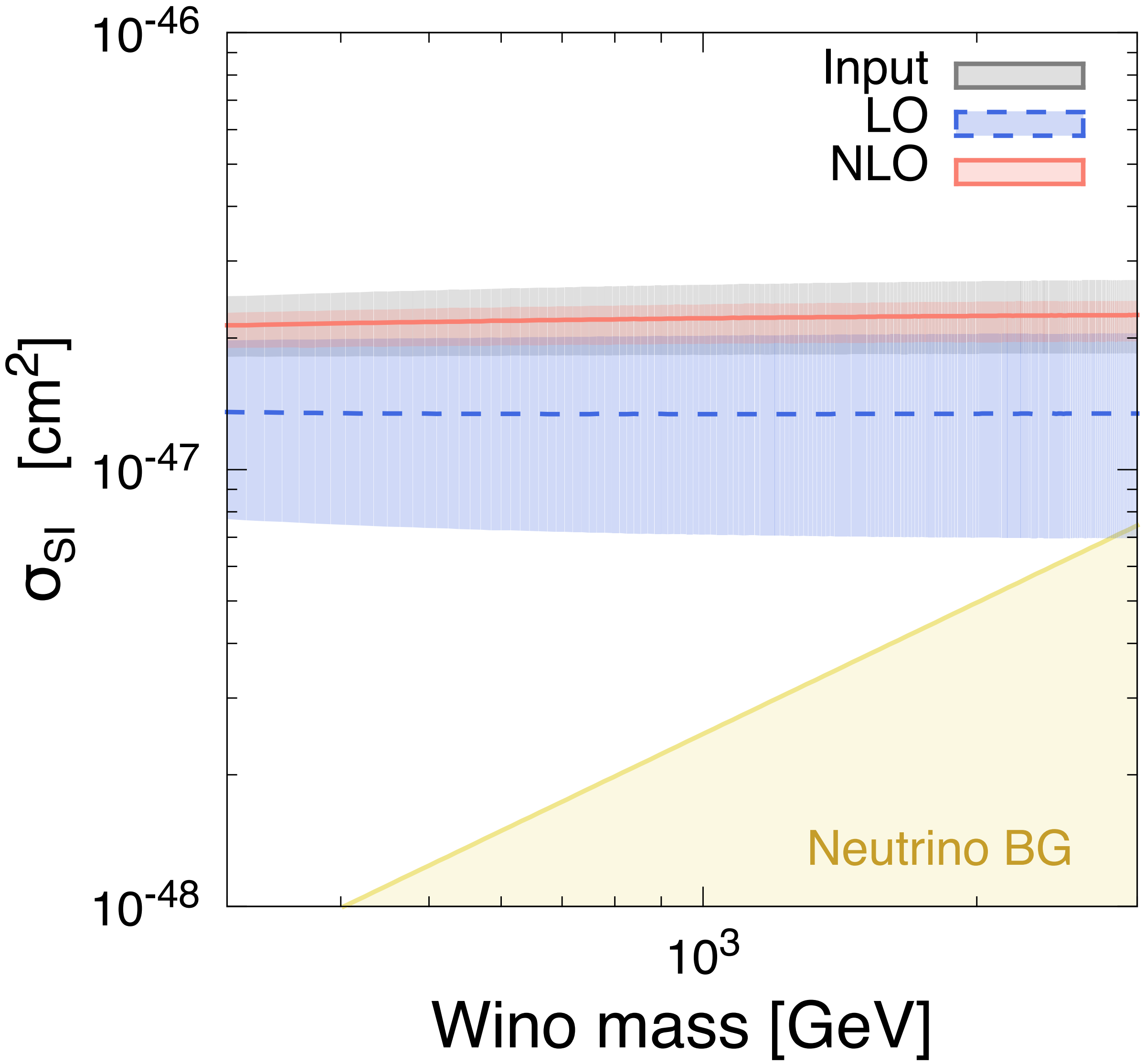

$$\sigma^p_{\rm SI} = 2.3\ ^{+0.2}_{-0.3}\ ^{+0.5}_{-0.4} \times 10^{-47}\ {\rm cm}^2$$

Current bounds for WIMP DM-nucleon cross section

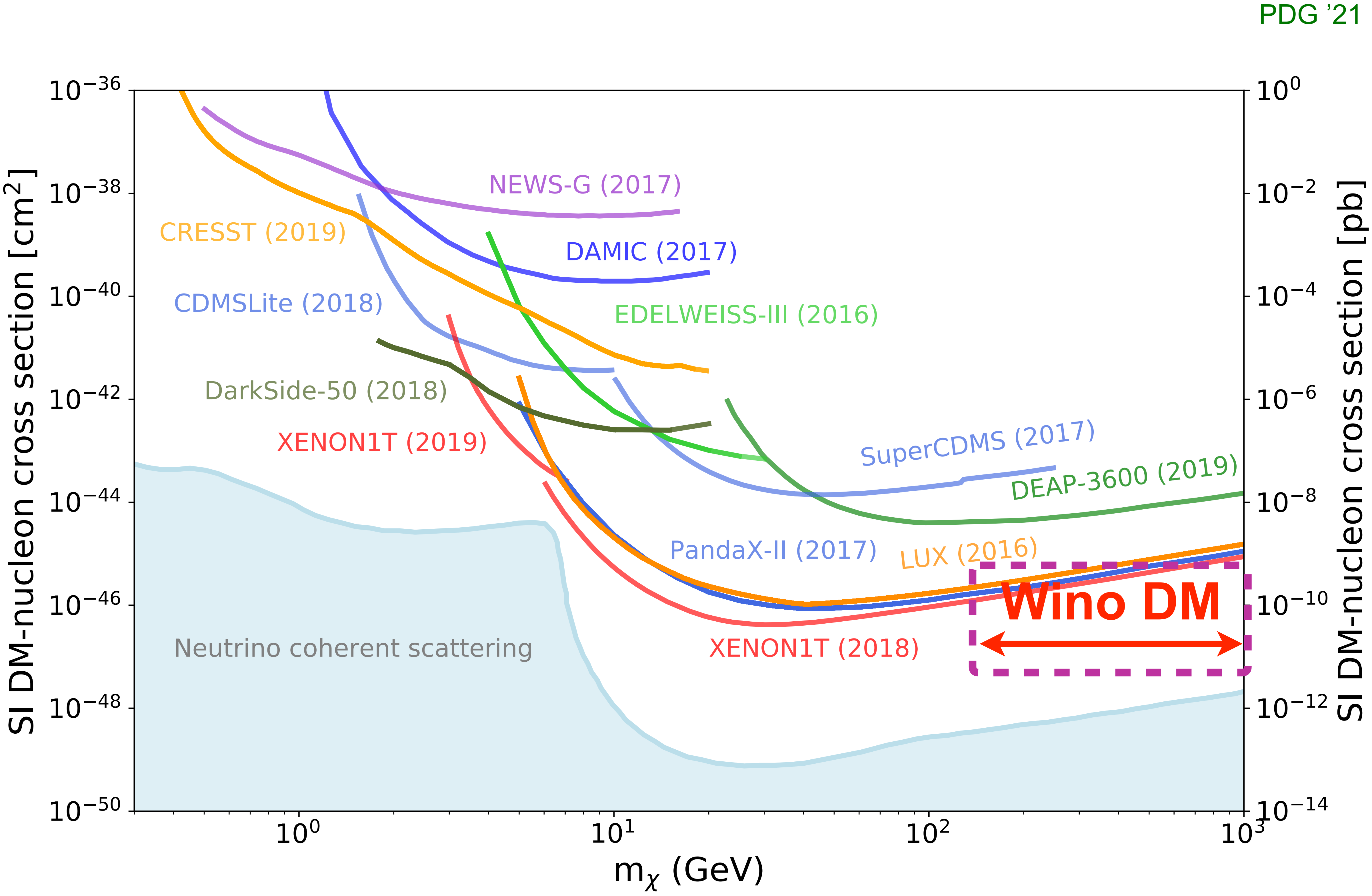

Future sensitivity

https://indico.cern.ch/event/765096/contributions/3295671/

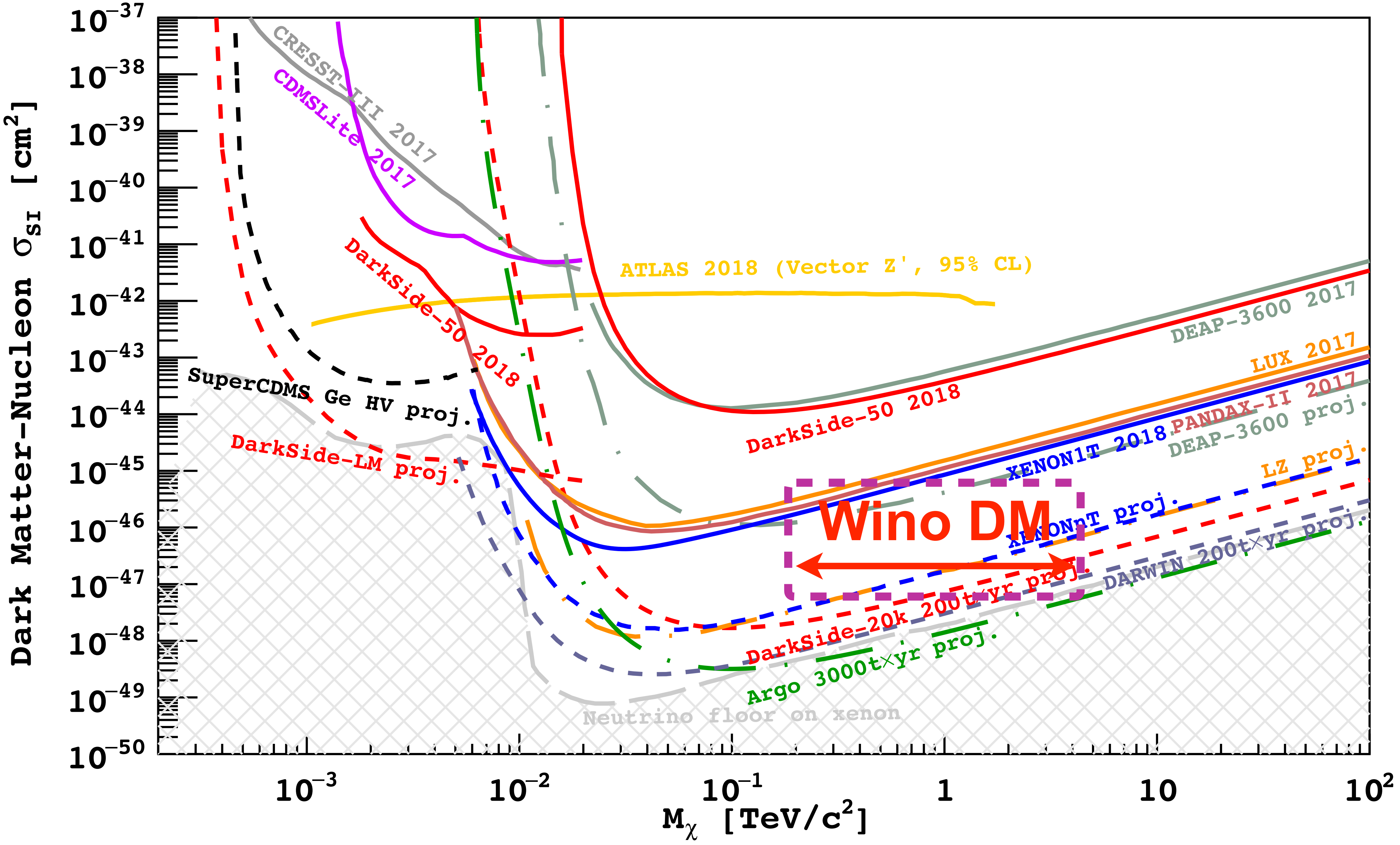

Features of the WIMP DM scenario

- DM abundance is naturally explained

- Promising theoretical models

  e.g.,

  Minimal supersymmetric extension of the SM (MSSM)

- It can be probed in **direct**/indirect detection experiments

Features of the WIMP DM scenario

- DM abundance is naturally explained

- Promising theoretical models

  e.g.,

  Minimal supersymmetric extension of the SM (MSSM)

- It can be probed in direct/**indirect** detection experiments

2. Indirect searches with dSphs

Indirect searches of WIMP DM

Target objects/regions for WIMP searches:

- Galactic center
- Extragalactic region
- Dwarf spheroidal galaxies

Stronger signals/Large astrophysical BGs

See, e.g.,

Lefranc et al. ’16

Rinchiuso et al.’18, ’20

Hryczuk et al. ’19

for the signals from the GC

Indirect searches of WIMP DM

Target objects/regions for WIMP searches:

- Galactic center
- Extragalactic region
- Dwarf spheroidal galaxies

Stronger signals/Large astrophysical BGs

See, e.g.,

Lefranc et al. ’16

Rinchiuso et al.’18, ’20

Hryczuk et al. ’19

for the signals from the GC

Dwarf spheroidal galaxies (dSphs)

- Satellite galaxies of a host galaxy
- No star formation

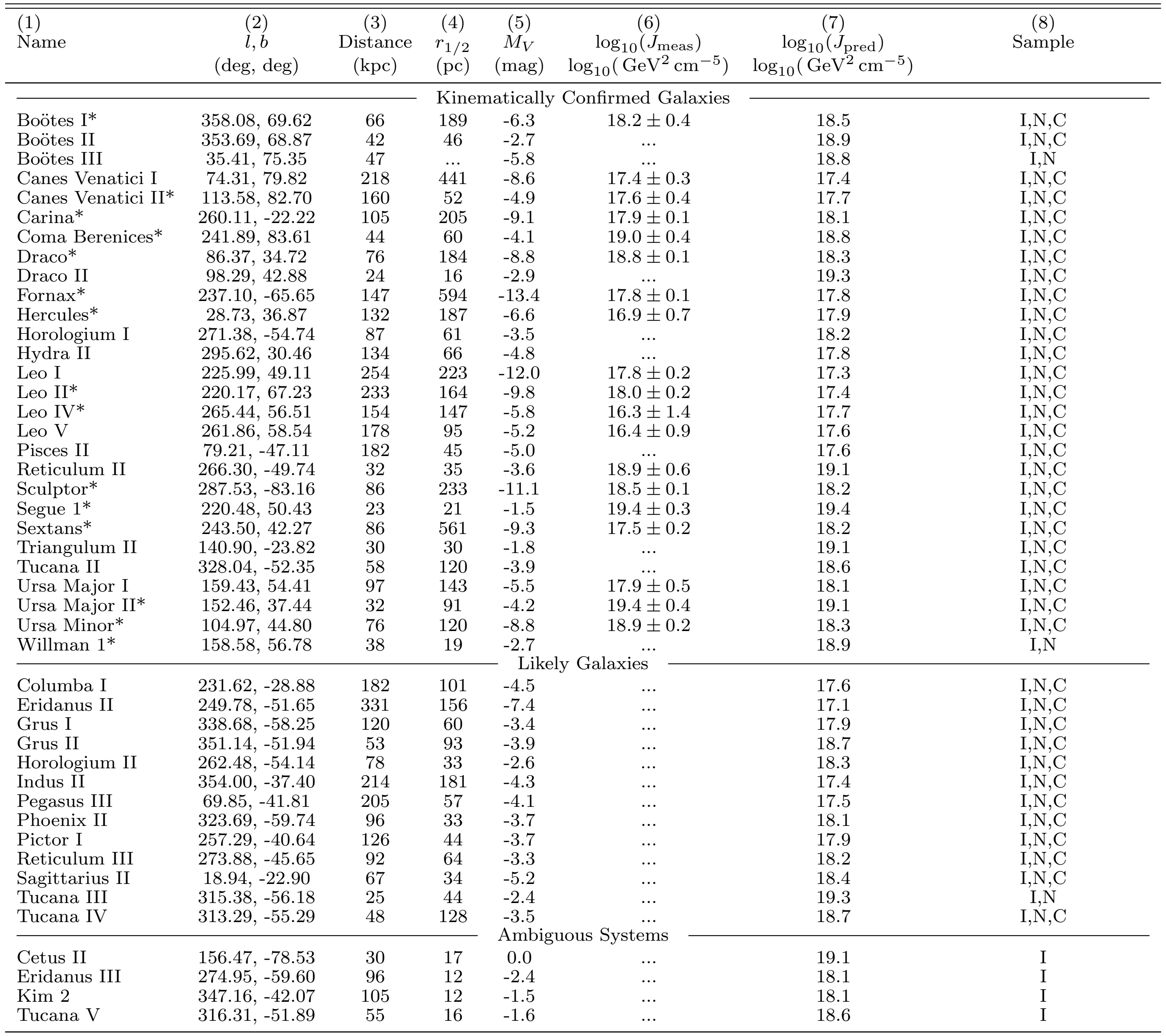

(1) Name	(2) l, b (deg, deg)	(3) Distance (kpc)	(4) $r_{1/2}$ (pc)	(5) M_V (mag)	(6) $\log_{10}(J_{\rm meas})$ $\log_{10}(\,{\rm GeV}^2\,{\rm cm}^{-5})$	(7) $\log_{10}(J_{\rm pred})$ $\log_{10}(\,{\rm GeV}^2\,{\rm cm}^{-5})$	(8) Sample
Kinematically Confirmed Galaxies							
Boötes I*	358.08, 69.62	66	189	-6.3	18.2 ± 0.4	18.5	I,N,C
Boötes II	353.69, 68.87	42	46	-2.7	...	18.9	I,N,C
Boötes III	35.41, 75.35	47	...	-5.8	...	18.8	I,N
Canes Venatici I	74.31, 79.82	218	441	-8.6	17.4 ± 0.3	17.4	I,N,C
Canes Venatici II*	113.58, 82.70	160	52	-4.9	17.6 ± 0.4	17.7	I,N,C
Carina*	260.11, -22.22	105	205	-9.1	17.9 ± 0.1	18.1	I,N,C
Coma Berenices*	241.89, 83.61	44	60	-4.1	19.0 ± 0.4	18.8	I,N,C
Draco*	86.37, 34.72	76	184	-8.8	18.8 ± 0.1	18.3	I,N,C
Draco II	98.29, 42.88	24	16	-2.9	...	19.3	I,N,C
Fornax*	237.10, -65.65	147	594	-13.4	17.8 ± 0.1	17.8	I,N,C
Hercules*	28.73, 36.87	132	187	-6.6	16.9 ± 0.7	17.9	I,N,C
Horologium I	271.38, -54.74	87	61	-3.5	...	18.2	I,N,C
Hydra II	295.62, 30.46	134	66	-4.8	...	17.8	I,N,C
Leo I	225.99, 49.11	254	223	-12.0	17.8 ± 0.2	17.3	I,N,C
Leo II*	220.17, 67.23	233	164	-9.8	18.0 ± 0.2	17.4	I,N,C
Leo IV*	265.44, 56.51	154	147	-5.8	16.3 ± 1.4	17.7	I,N,C
Leo V	261.86, 58.54	178	95	-5.2	16.4 ± 0.9	17.6	I,N,C
Pisces II	79.21, -47.11	182	45	-5.0	...	17.6	I,N,C
Reticulum II	266.30, -49.74	32	35	-3.6	18.9 ± 0.6	19.1	I,N,C
Sculptor*	287.53, -83.16	86	233	-11.1	18.5 ± 0.1	18.2	I,N,C
Segue 1*	220.48, 50.43	23	21	-1.5	19.4 ± 0.3	19.4	I,N,C
Sextans*	243.50, 42.27	86	561	-9.3	17.5 ± 0.2	18.2	I,N,C
Triangulum II	140.90, -23.82	30	30	-1.8	...	19.1	I,N,C
Tucana II	328.04, -52.35	58	120	-3.9	...	18.6	I,N,C
Ursa Major I	159.43, 54.41	97	143	-5.5	17.9 ± 0.5	18.1	I,N,C
Ursa Major II*	152.46, 37.44	32	91	-4.2	19.4 ± 0.4	19.1	I,N,C
Ursa Minor*	104.97, 44.80	76	120	-8.8	18.9 ± 0.2	18.3	I,N,C
Willman 1*	158.58, 56.78	38	19	-2.7	...	18.9	I,N
Likely Galaxies							
Columba I	231.62, -28.88	182	101	-4.5	...	17.6	I,N,C
Eridanus II	249.78, -51.65	331	156	-7.4	...	17.1	I,N,C
Grus I	338.68, -58.25	120	60	-3.4	...	17.9	I,N,C
Grus II	351.14, -51.94	53	93	-3.9	...	18.7	I,N,C
Horologium II	262.48, -54.14	78	33	-2.6	...	18.3	I,N,C
Indus II	354.00, -37.40	214	181	-4.3	...	17.4	I,N,C
Pegasus III	69.85, -41.81	205	57	-4.1	...	17.5	I,N,C
Phoenix II	323.69, -59.74	96	33	-3.7	...	18.1	I,N,C
Pictor I	257.29, -40.64	126	44	-3.7	...	17.9	I,N,C
Reticulum III	273.88, -45.65	92	64	-3.3	...	18.2	I,N,C
Sagittarius II	18.94, -22.90	67	34	-5.2	...	18.4	I,N,C
Tucana III	315.38, -56.18	25	44	-2.4	...	19.3	I,N
Tucana IV	313.29, -55.29	48	128	-3.5	...	18.7	I,N,C
Ambiguous Systems							
Cetus II	156.47, -78.53	30	17	0.0	...	19.1	I
Eridanus III	274.95, -59.60	96	12	-2.4	...	18.1	I
Kim 2	347.16, -42.07	105	12	-1.5	...	18.1	I
Tucana V	316.31, -51.89	55	16	-1.6	...	18.6	I

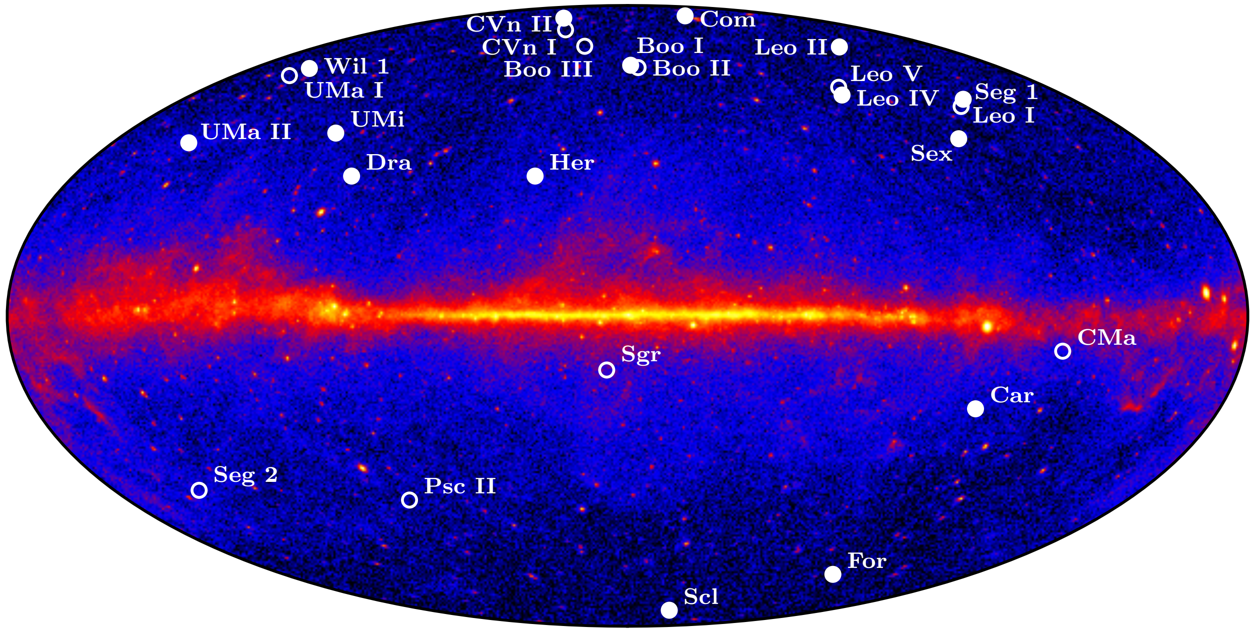

Ackermann et al. ’13

Albert et al. ’16

Dwarf spheroidal galaxies (dSphs)

- Satellite galaxies of a host galaxy
- No star formation

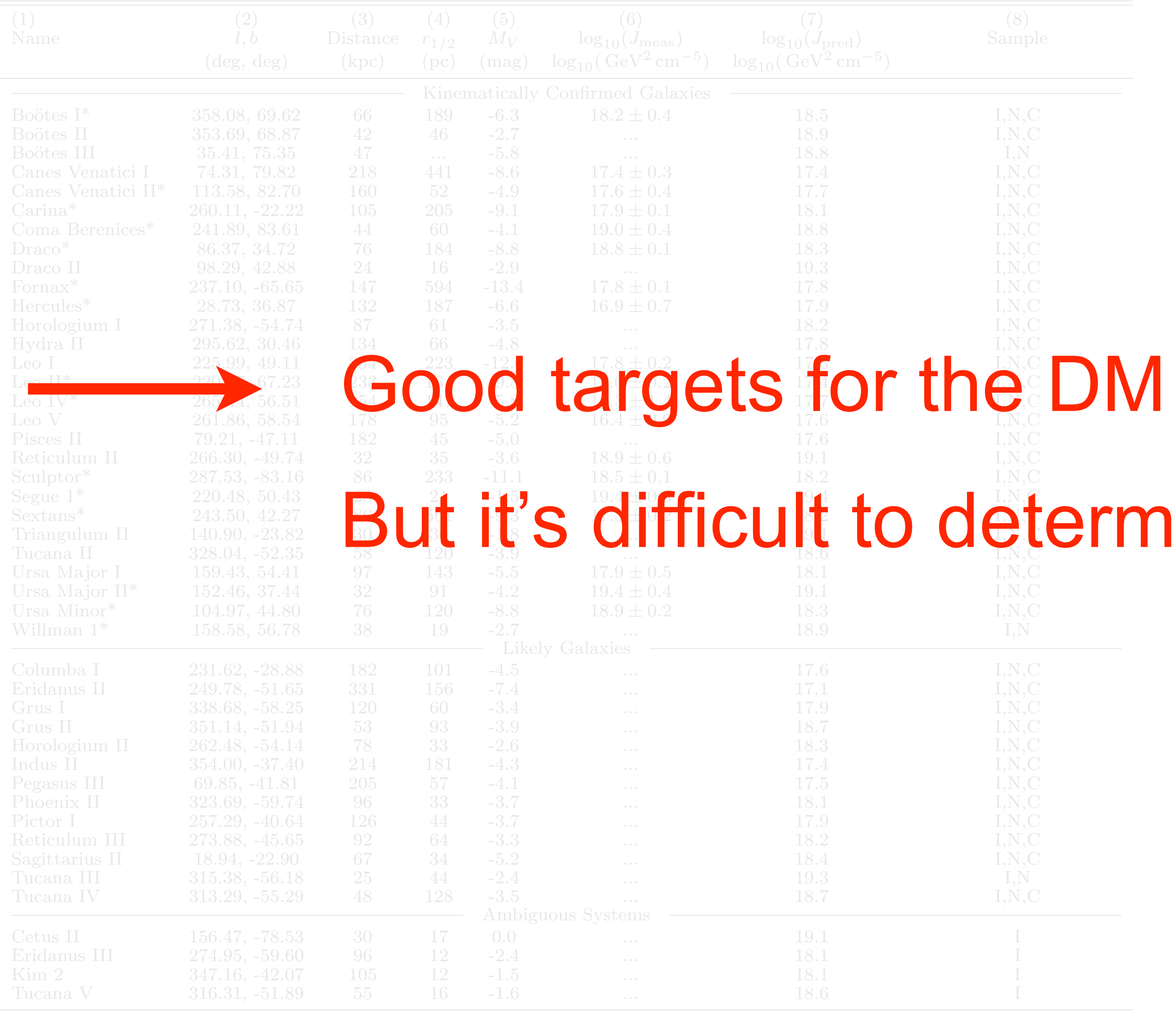

(1) Name	(2) l, b (deg, deg)	(3) Distance (kpc)	(4) $r_{1/2}$ (pc)	(5) M_V (mag)	(6) $\log_{10}(J_{\rm meas})$ $\log_{10}(\,{\rm GeV}^2\,{\rm cm}^{-5})$	(7) $\log_{10}(J_{\rm pred})$ $\log_{10}(\,{\rm GeV}^2\,{\rm cm}^{-5})$	(8) Sample
			Kinematically Confirmed Galaxies				
Boötes I*	358.08, 69.62	66	189	-6.3	18.2 ± 0.4	18.5	I,N,C
Boötes II	353.69, 68.87	42	46	-2.7	...	18.9	I,N,C
Boötes III	35.41, 75.35	47	...	-5.8	...	18.8	I,N
Canes Venatici I	74.31, 79.82	218	441	-8.6	17.4 ± 0.3	17.4	I,N,C
Canes Venatici II*	113.58, 82.70	160	52	-4.9	17.6 ± 0.4	17.7	I,N,C
Carina*	260.11, -22.22	105	205	-9.1	17.9 ± 0.1	18.1	I,N,C
Coma Berenices*	241.89, 83.61	44	60	-4.1	19.0 ± 0.4	18.8	I,N,C
Draco*	86.37, 34.72	76	184	-8.8	18.8 ± 0.1	18.3	I,N,C
Draco II	98.29, 42.88	24	16	-2.9	...	19.3	I,N,C
Fornax*	237.10, -65.65	147	594	-13.4	17.8 ± 0.1	17.8	I,N,C
Hercules*	28.73, 36.87	132	187	-6.6	16.9 ± 0.7	17.9	I,N,C
Horologium I	271.38, -54.74	87	61	-3.5	...	18.2	I,N,C
Hydra II	295.62, 30.46	134	66	-4.8	...	17.8	I,N,C
Leo I	225.99, 49.11	[illegible]	223	[illegible]	17.8 ± 0.2	[illegible]	I,N,C
Leo II*	[illegible]	[illegible]	[illegible]	[illegible]	[illegible]	[illegible]	[illegible]
Leo IV*	[illegible]	[illegible]	[illegible]	[illegible]	[illegible]	[illegible]	[illegible]
Leo V	261.86, 58.54	178	95	-5.2	[illegible]	17.6	I,N,C
Pisces II	79.21, -47.11	182	45	-5.0	...	17.6	I,N,C
Reticulum II	266.30, -49.74	32	35	-3.6	18.9 ± 0.6	19.1	I,N,C
Sculptor*	287.53, -83.16	86	233	-11.1	18.5 ± 0.1	18.2	I,N,C
Segue 1*	220.48, 50.43	[illegible]	[illegible]	[illegible]	[illegible]	[illegible]	[illegible]
Sextans*	243.50, 42.27	[illegible]	[illegible]	[illegible]	[illegible]	[illegible]	[illegible]
Triangulum II	140.90, -23.82	[illegible]	[illegible]	[illegible]	[illegible]	[illegible]	[illegible]
Tucana II	328.04, -52.35	58	120	-3.9	...	18.6	I,N,C
Ursa Major I	159.43, 54.41	97	143	-5.5	17.9 ± 0.5	18.1	I,N,C
Ursa Major II*	152.46, 37.44	32	91	-4.2	19.4 ± 0.4	19.1	I,N,C
Ursa Minor*	104.97, 44.80	76	120	-8.8	18.9 ± 0.2	18.3	I,N,C
Willman 1*	158.58, 56.78	38	19	-2.7	...	18.9	I,N
			Likely Galaxies				
Columba I	231.62, -28.88	182	101	-4.5	...	17.6	I,N,C
Eridanus II	249.78, -51.65	331	156	-7.4	...	17.1	I,N,C
Grus I	338.68, -58.25	120	60	-3.4	...	17.9	I,N,C
Grus II	351.14, -51.94	53	93	-3.9	...	18.7	I,N,C
Horologium II	262.48, -54.14	78	33	-2.6	...	18.3	I,N,C
Indus II	354.00, -37.40	214	181	-4.3	...	17.4	I,N,C
Pegasus III	69.85, -41.81	205	57	-4.1	...	17.5	I,N,C
Phoenix II	323.69, -59.74	96	33	-3.7	...	18.1	I,N,C
Pictor I	257.29, -40.64	126	44	-3.7	...	17.9	I,N,C
Reticulum III	273.88, -45.65	92	64	-3.3	...	18.2	I,N,C
Sagittarius II	18.94, -22.90	67	34	-5.2	...	18.4	I,N,C
Tucana III	315.38, -56.18	25	44	-2.4	...	19.3	I,N
Tucana IV	313.29, -55.29	48	128	-3.5	...	18.7	I,N,C
			Ambiguous Systems				
Cetus II	156.47, -78.53	30	17	0.0	...	19.1	I
Eridanus III	274.95, -59.60	96	12	-2.4	...	18.1	I
Kim 2	347.16, -42.07	105	12	-1.5	...	18.1	I
Tucana V	316.31, -51.89	55	16	-1.6	...	18.6	I

Good targets for the DM search

But it's difficult to determine their properties

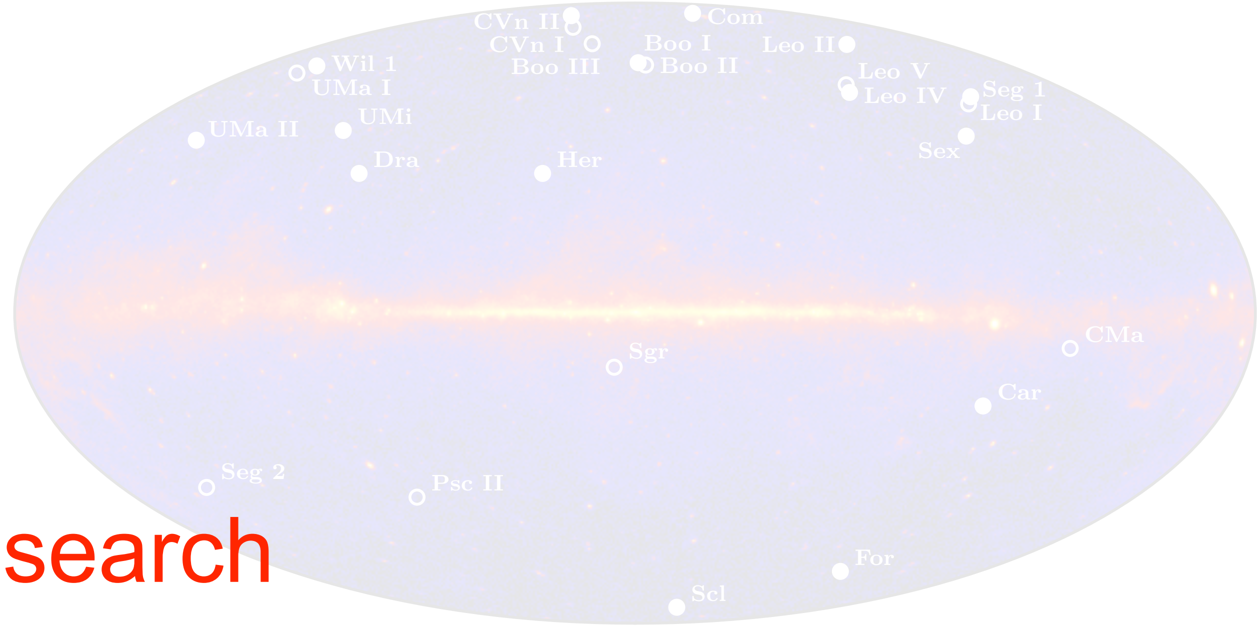

Ackermann et al. '13

Albert et al. '16

Gamma-ray flux from dSphs

$$\frac{d\Phi_\gamma}{dE} = J(\theta)\frac{\sigma v}{8\pi m_{\rm dm}^2}\frac{dN_\gamma}{dE}$$

See Ando, KI ’21

Boddy et al. ’17

Lu et al. ’18

Petac et al. ’18

Bergstrom et al. ’18

and Jason Kumar’s talk

for a case where the cross section is velocity dependent

Gamma-ray flux from dSphs

$$\frac{d\Phi_\gamma}{dE} = \boxed{J(\theta)}\,\boxed{\frac{\sigma v}{8\pi m_{\rm dm}^2}\frac{dN_\gamma}{dE}}$$

J-factor
(depending on dSphs)

DM model

See Ando, KI ’21
Boddy et al. ’17
Lu et al. ’18
Petac et al. ’18
Bergstrom et al. ’18
and Jason Kumar’s talk
for a case where the cross section is velocity dependent

Gamma-ray flux from dSphs

$$\frac{d\Phi_\gamma}{dE} = \boxed{J(\theta)}\,\boxed{\frac{\sigma v}{8\pi m_{\rm dm}^2}\frac{dN_\gamma}{dE}}$$

J-factor
(depending on dSphs)

DM model

See Ando, KI ’21
Boddy et al. ’17
Lu et al. ’18
Petac et al. ’18
Bergstrom et al. ’18
and Jason Kumar’s talk
for a case where the cross section is velocity dependent

J-factor

$$J(\theta) = \int_{\text{l.o.s.}(\theta)} d\ell \, \boxed{\rho^2(\vec{x})}$$

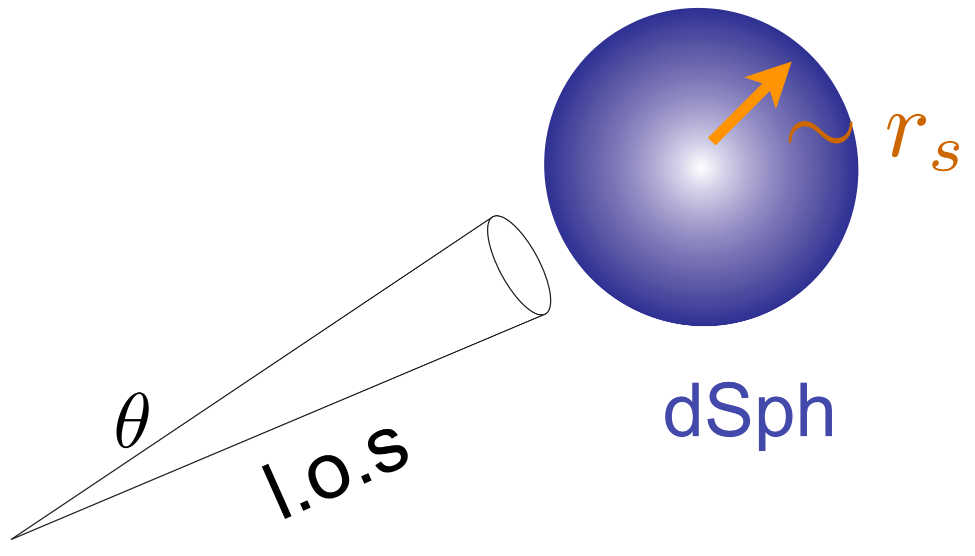

NFW profile

$$\rho(r) = \begin{cases} \boxed{\frac{\rho_s}{(r/r_s)(1+r/r_s)^2}} & r < r_t \\ 0 & r > r_t \end{cases}$$

ρ_s : energy density
r_s : radius
r_t : truncation radius

Parameters that characterize dSphs

Measured properties of dSphs

D : distance

θ_h : projected angular half-light radius

$\sigma_{\rm los}$: l.o.s velocity dispersion

cf.

ρ_s : energy density

r_s : radius

r_t : truncation radius

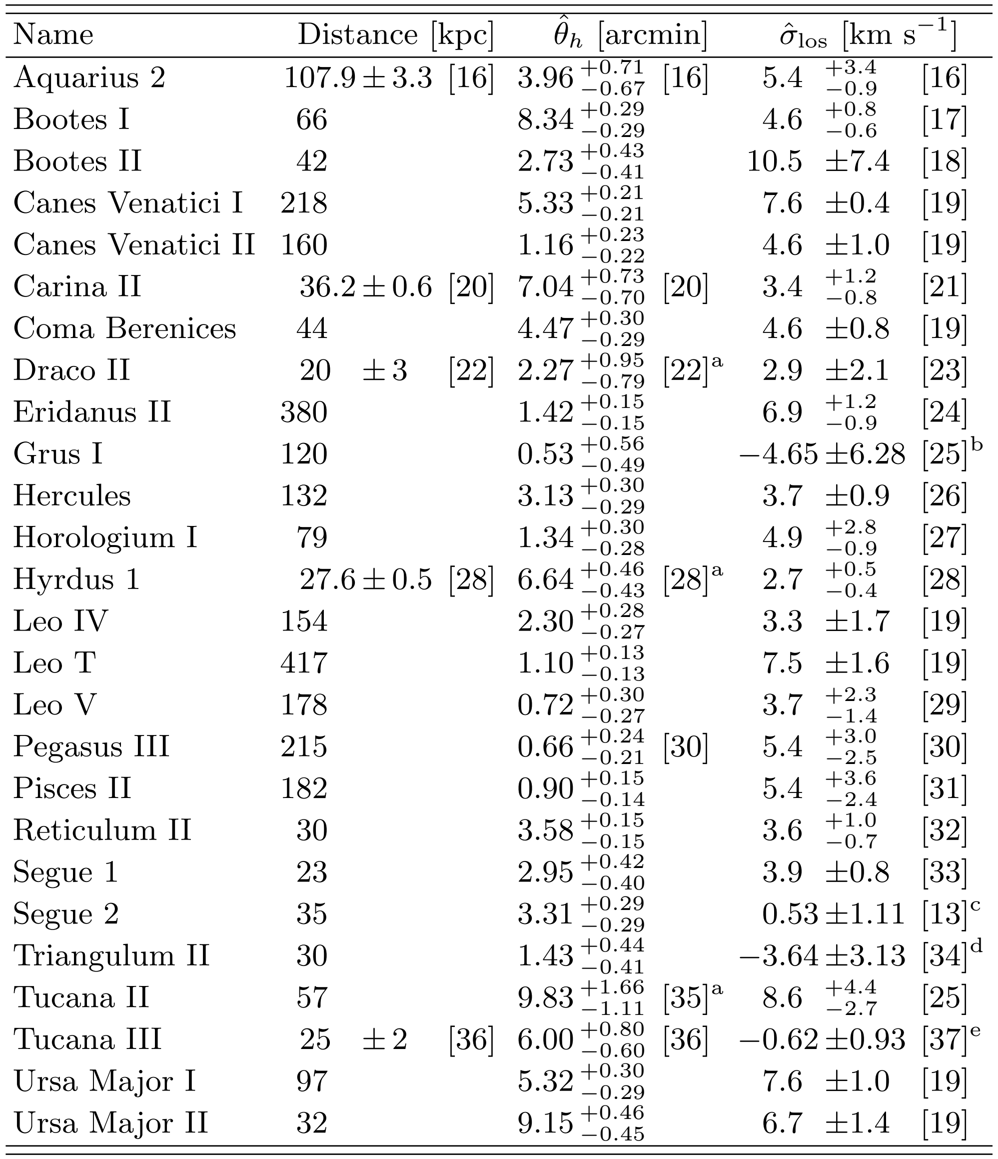

Name	Distance [kpc]		$\hat{\theta}_h$ [arcmin]		$\hat{\sigma}_{\rm los}$ [km s^{-1}]	
Aquarius 2	107.9 ± 3.3	[16]	$3.96^{+0.71}_{-0.67}$	[16]	$5.4^{+3.4}_{-0.9}$	[16]
Bootes I	66		$8.34^{+0.29}_{-0.29}$		$4.6^{+0.8}_{-0.6}$	[17]
Bootes II	42		$2.73^{+0.43}_{-0.41}$		10.5 ± 7.4	[18]
Canes Venatici I	218		$5.33^{+0.21}_{-0.21}$		7.6 ± 0.4	[19]
Canes Venatici II	160		$1.16^{+0.23}_{-0.22}$		4.6 ± 1.0	[19]
Carina II	36.2 ± 0.6	[20]	$7.04^{+0.73}_{-0.70}$	[20]	$3.4^{+1.2}_{-0.8}$	[21]
Coma Berenices	44		$4.47^{+0.30}_{-0.29}$		4.6 ± 0.8	[19]
Draco II	20 ± 3	[22]	$2.27^{+0.95}_{-0.79}$	[22]$^{\rm a}$	2.9 ± 2.1	[23]
Eridanus II	380		$1.42^{+0.15}_{-0.15}$		$6.9^{+1.2}_{-0.9}$	[24]
Grus I	120		$0.53^{+0.56}_{-0.49}$		-4.65 ± 6.28	[25]$^{\rm b}$
Hercules	132		$3.13^{+0.30}_{-0.29}$		3.7 ± 0.9	[26]
Horologium I	79		$1.34^{+0.30}_{-0.28}$		$4.9^{+2.8}_{-0.9}$	[27]
Hyrdus 1	27.6 ± 0.5	[28]	$6.64^{+0.46}_{-0.43}$	[28]$^{\rm a}$	$2.7^{+0.5}_{-0.4}$	[28]
Leo IV	154		$2.30^{+0.28}_{-0.27}$		3.3 ± 1.7	[19]
Leo T	417		$1.10^{+0.13}_{-0.13}$		7.5 ± 1.6	[19]
Leo V	178		$0.72^{+0.30}_{-0.27}$		$3.7^{+2.3}_{-1.4}$	[29]
Pegasus III	215		$0.66^{+0.24}_{-0.21}$	[30]	$5.4^{+3.0}_{-2.5}$	[30]
Pisces II	182		$0.90^{+0.15}_{-0.14}$		$5.4^{+3.6}_{-2.4}$	[31]
Reticulum II	30		$3.58^{+0.15}_{-0.15}$		$3.6^{+1.0}_{-0.7}$	[32]
Segue 1	23		$2.95^{+0.42}_{-0.40}$		3.9 ± 0.8	[33]
Segue 2	35		$3.31^{+0.29}_{-0.29}$		0.53 ± 1.11	[13]$^{\rm c}$
Triangulum II	30		$1.43^{+0.44}_{-0.41}$		-3.64 ± 3.13	[34]$^{\rm d}$
Tucana II	57		$9.83^{+1.66}_{-1.11}$	[35]$^{\rm a}$	$8.6^{+4.4}_{-2.7}$	[25]
Tucana III	25 ± 2	[36]	$6.00^{+0.80}_{-0.60}$	[36]	-0.62 ± 0.93	[37]$^{\rm e}$
Ursa Major I	97		$5.32^{+0.30}_{-0.29}$		7.6 ± 1.0	[19]
Ursa Major II	32		$9.15^{+0.46}_{-0.45}$		6.7 ± 1.4	[19]

Ando et al. ’20

Measured properties of dSphs

D : distance

θ_h : projected angular half-light radius

$\sigma_{\rm los}$: l.o.s velocity dispersion

cf.

ρ_s : energy density

r_s : radius

r_t : truncation radius

How do we use the observed quantities?

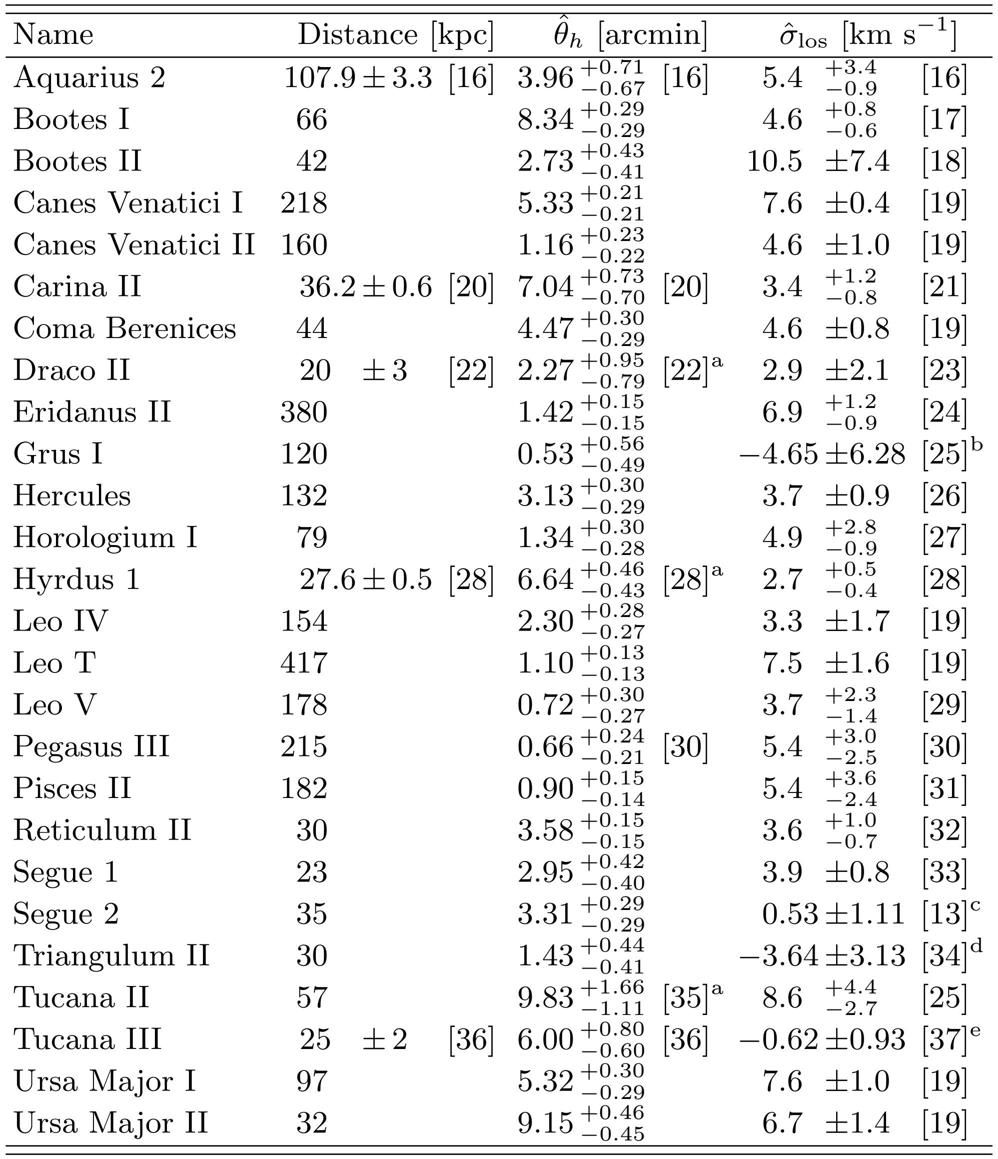

Name	Distance [kpc]		$\hat{\theta}_h$ [arcmin]		$\hat{\sigma}_{\rm los}$ [km s^{-1}]	
Aquarius 2	107.9 ± 3.3	[16]	$3.96^{+0.71}_{-0.67}$	[16]	$5.4^{+3.4}_{-0.9}$	[16]
Bootes I	66		$8.34^{+0.29}_{-0.29}$		$4.6^{+0.8}_{-0.6}$	[17]
Bootes II	42		$2.73^{+0.43}_{-0.41}$		10.5 ± 7.4	[18]
Canes Venatici I	218		$5.33^{+0.21}_{-0.21}$		7.6 ± 0.4	[19]
Canes Venatici II	160		$1.16^{+0.23}_{-0.22}$		4.6 ± 1.0	[19]
Carina II	36.2 ± 0.6	[20]	$7.04^{+0.73}_{-0.70}$	[20]	$3.4^{+1.2}_{-0.8}$	[21]
Coma Berenices	44		$4.47^{+0.30}_{-0.29}$		4.6 ± 0.8	[19]
Draco II	20 ± 3	[22]	$2.27^{+0.95}_{-0.79}$	[22]$^{\rm a}$	2.9 ± 2.1	[23]
Eridanus II	380		$1.42^{+0.15}_{-0.15}$		$6.9^{+1.2}_{-0.9}$	[24]
Grus I	120		$0.53^{+0.56}_{-0.49}$		-4.65 ± 6.28	[25]$^{\rm b}$
Hercules	132		$3.13^{+0.30}_{-0.29}$		3.7 ± 0.9	[26]
Horologium I	79		$1.34^{+0.30}_{-0.28}$		$4.9^{+2.8}_{-0.9}$	[27]
Hyrdus 1	27.6 ± 0.5	[28]	$6.64^{+0.46}_{-0.43}$	[28]$^{\rm a}$	$2.7^{+0.5}_{-0.4}$	[28]
Leo IV	154		$2.30^{+0.28}_{-0.27}$		3.3 ± 1.7	[19]
Leo T	417		$1.10^{+0.13}_{-0.13}$		7.5 ± 1.6	[19]
Leo V	178		$0.72^{+0.30}_{-0.27}$		$3.7^{+2.3}_{-1.4}$	[29]
Pegasus III	215		$0.66^{+0.24}_{-0.21}$	[30]	$5.4^{+3.0}_{-2.5}$	[30]
Pisces II	182		$0.90^{+0.15}_{-0.14}$		$5.4^{+3.6}_{-2.4}$	[31]
Reticulum II	30		$3.58^{+0.15}_{-0.15}$		$3.6^{+1.0}_{-0.7}$	[32]
Segue 1	23		$2.95^{+0.42}_{-0.40}$		3.9 ± 0.8	[33]
Segue 2	35		$3.31^{+0.29}_{-0.29}$		0.53 ± 1.11	[13]$^{\rm c}$
Triangulum II	30		$1.43^{+0.44}_{-0.41}$		-3.64 ± 3.13	[34]$^{\rm d}$
Tucana II	57		$9.83^{+1.66}_{-1.11}$	[35]$^{\rm a}$	$8.6^{+4.4}_{-2.7}$	[25]
Tucana III	25 ± 2	[36]	$6.00^{+0.80}_{-0.60}$	[36]	-0.62 ± 0.93	[37]$^{\rm e}$
Ursa Major I	97		$5.32^{+0.30}_{-0.29}$		7.6 ± 1.0	[19]
Ursa Major II	32		$9.15^{+0.46}_{-0.45}$		6.7 ± 1.4	[19]

Ando et al. ’20

Measured properties of dSphs

D : distance

θ_h : projected angular half-light radius

$\sigma_{\rm los}$: l.o.s velocity dispersion

↓

cf.

ρ_s : energy density

r_s : radius

r_t : truncation radius

How do we use the observed quantities?

Name	Distance [kpc]		$\hat{\theta}_h$ [arcmin]		$\hat{\sigma}_{\rm los}$ [km s^{-1}]	
Aquarius 2	107.9 ± 3.3	[16]	$3.96^{+0.71}_{-0.67}$	[16]	$5.4^{+3.4}_{-0.9}$	[16]
Bootes I	66		$8.34^{+0.29}_{-0.29}$		$4.6^{+0.8}_{-0.6}$	[17]
Bootes II	42		$2.73^{+0.43}_{-0.41}$		10.5 ± 7.4	[18]
Canes Venatici I	218		$5.33^{+0.21}_{-0.21}$		7.6 ± 0.4	[19]
Canes Venatici II	160		$1.16^{+0.23}_{-0.22}$		4.6 ± 1.0	[19]
Carina II	36.2 ± 0.6	[20]	$7.04^{+0.73}_{-0.70}$	[20]	$3.4^{+1.2}_{-0.8}$	[21]
Coma Berenices	44		$4.47^{+0.30}_{-0.29}$		4.6 ± 0.8	[19]
Draco II	20 ± 3	[22]	$2.27^{+0.95}_{-0.79}$	[22][a]	2.9 ± 2.1	[23]
Eridanus II	380		$1.42^{+0.15}_{-0.15}$		$6.9^{+1.2}_{-0.9}$	[24]
Grus I	120		$0.53^{+0.56}_{-0.49}$		-4.65 ± 6.28	[25][b]
Hercules	132		$3.13^{+0.30}_{-0.29}$		3.7 ± 0.9	[26]
Horologium I	79		$1.34^{+0.30}_{-0.28}$		$4.9^{+2.8}_{-0.9}$	[27]
Hyrdus 1	27.6 ± 0.5	[28]	$6.64^{+0.46}_{-0.43}$	[28][a]	$2.7^{+0.5}_{-0.4}$	[28]
Leo IV	154		$2.30^{+0.28}_{-0.27}$		3.3 ± 1.7	[19]
Leo T	417		$1.10^{+0.13}_{-0.13}$		7.5 ± 1.6	[19]
Leo V	178		$0.72^{+0.30}_{-0.27}$		$3.7^{+2.3}_{-1.4}$	[29]
Pegasus III	215		$0.66^{+0.24}_{-0.21}$	[30]	$5.4^{+3.0}_{-2.5}$	[30]
Pisces II	182		$0.90^{+0.15}_{-0.14}$		$5.4^{+3.6}_{-2.4}$	[31]
Reticulum II	30		$3.58^{+0.15}_{-0.15}$		$3.6^{+1.0}_{-0.7}$	[32]
Segue 1	23		$2.95^{+0.42}_{-0.40}$		3.9 ± 0.8	[33]
Segue 2	35		$3.31^{+0.29}_{-0.29}$		0.53 ± 1.11	[13][c]
Triangulum II	30		$1.43^{+0.44}_{-0.41}$		-3.64 ± 3.13	[34][d]
Tucana II	57		$9.83^{+1.66}_{-1.11}$	[35][a]	$8.6^{+4.4}_{-2.7}$	[25]
Tucana III	25 ± 2	[36]	$6.00^{+0.80}_{-0.60}$	[36]	-0.62 ± 0.93	[37][e]
Ursa Major I	97		$5.32^{+0.30}_{-0.29}$		7.6 ± 1.0	[19]
Ursa Major II	32		$9.15^{+0.46}_{-0.45}$		6.7 ± 1.4	[19]

Ando et al. ’20

We’re going to take a theoretical approach

See Alvarez et al. ’20
for data driven-approach

Formation of dSphs

Density fluctuation

↓

Halos (including subhalos)

↓

Subhalos accrete on a host halo

↓

Satellite galaxies formed in the host halo

dSphs

Formation of dSphs

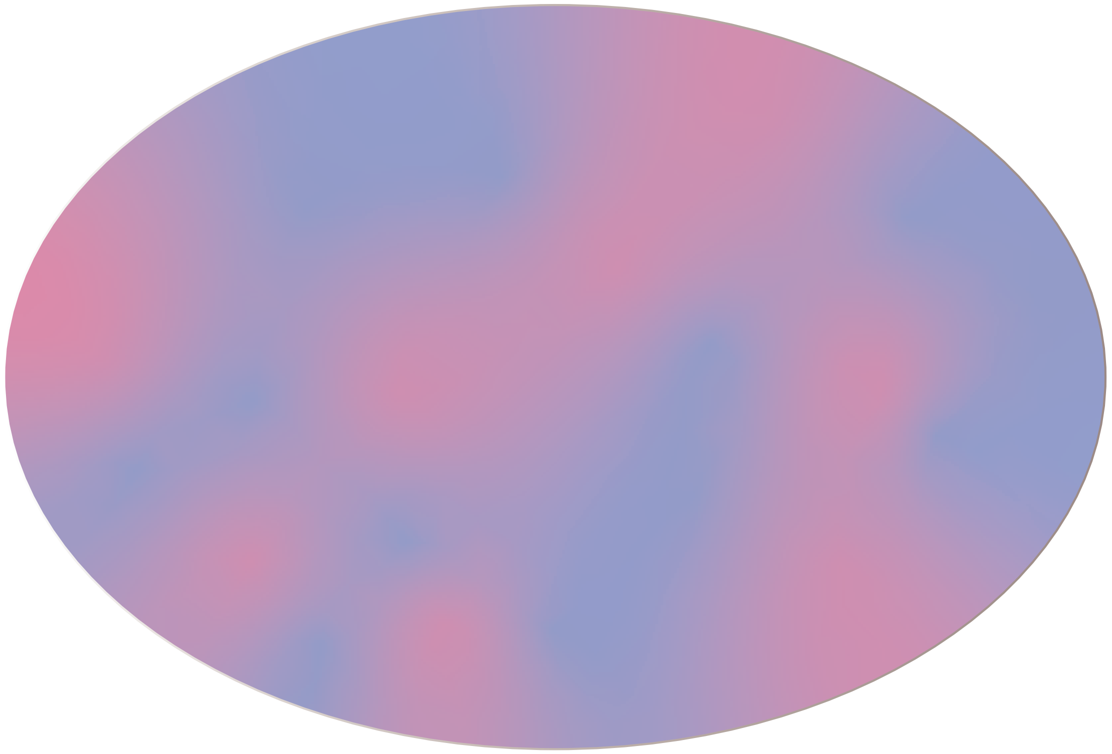

Density fluctuation

↓

Halos (including subhalos)

↓

Subhalos accrete on a host halo

↓

Satellite galaxies formed in the host halo

dSphs

Formation of dSphs

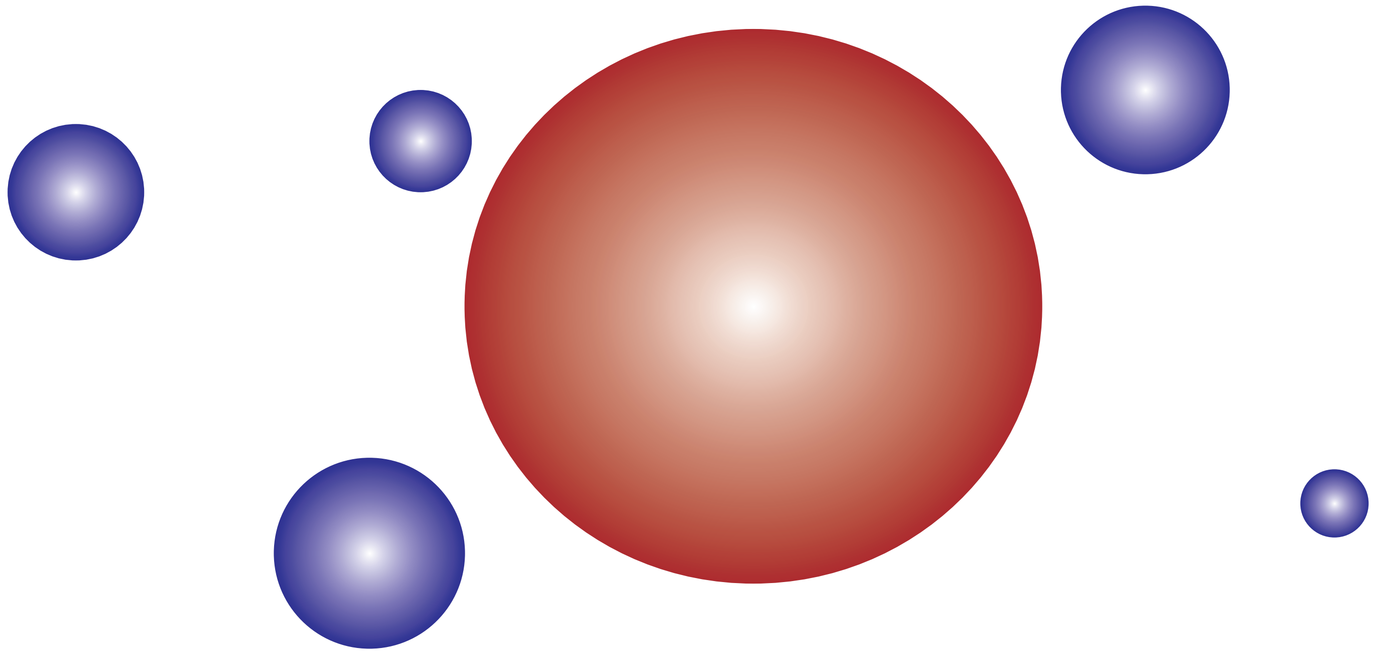

Density fluctuation

↓

Halos (including subhalos)

↓

Subhalos accrete on a host halo

↓

Satellite galaxies formed in the host halo

dSphs

Formation of dSphs

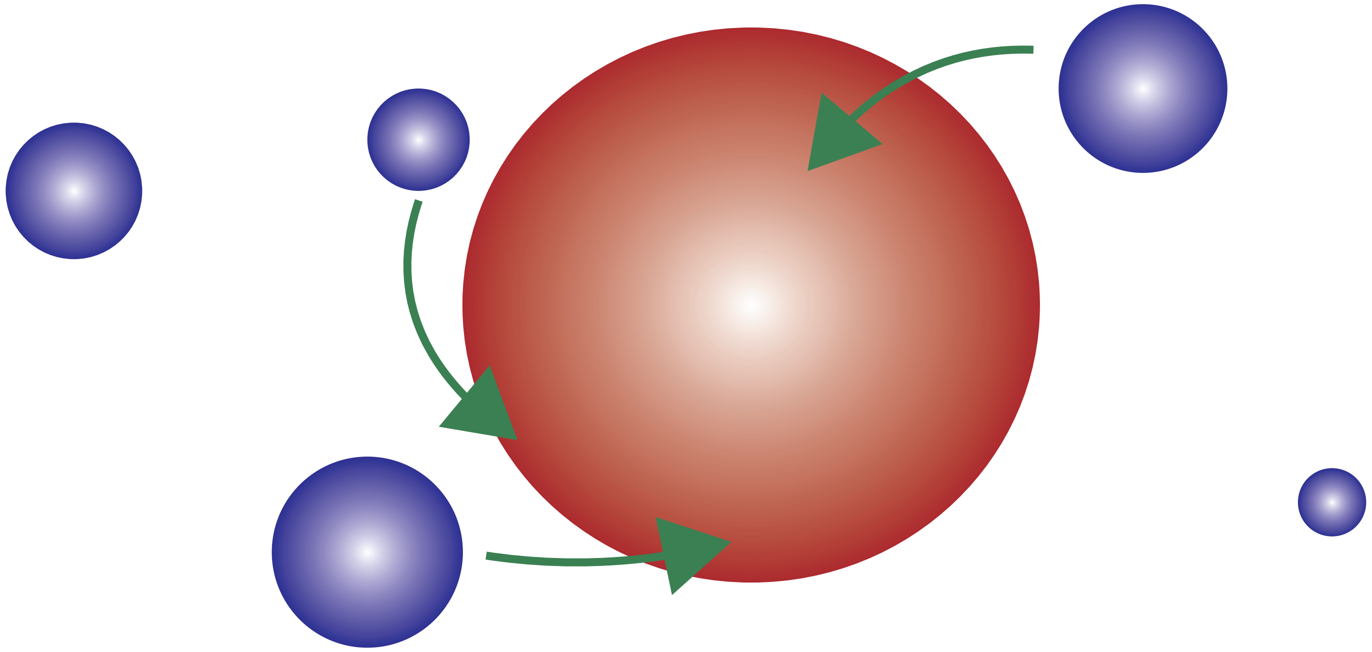

Density fluctuation

↓

Halos (including subhalos)

↓

Subhalos accrete on a host halo

↓

Satellite galaxies formed in the host halo

dSphs

Formation of dSphs

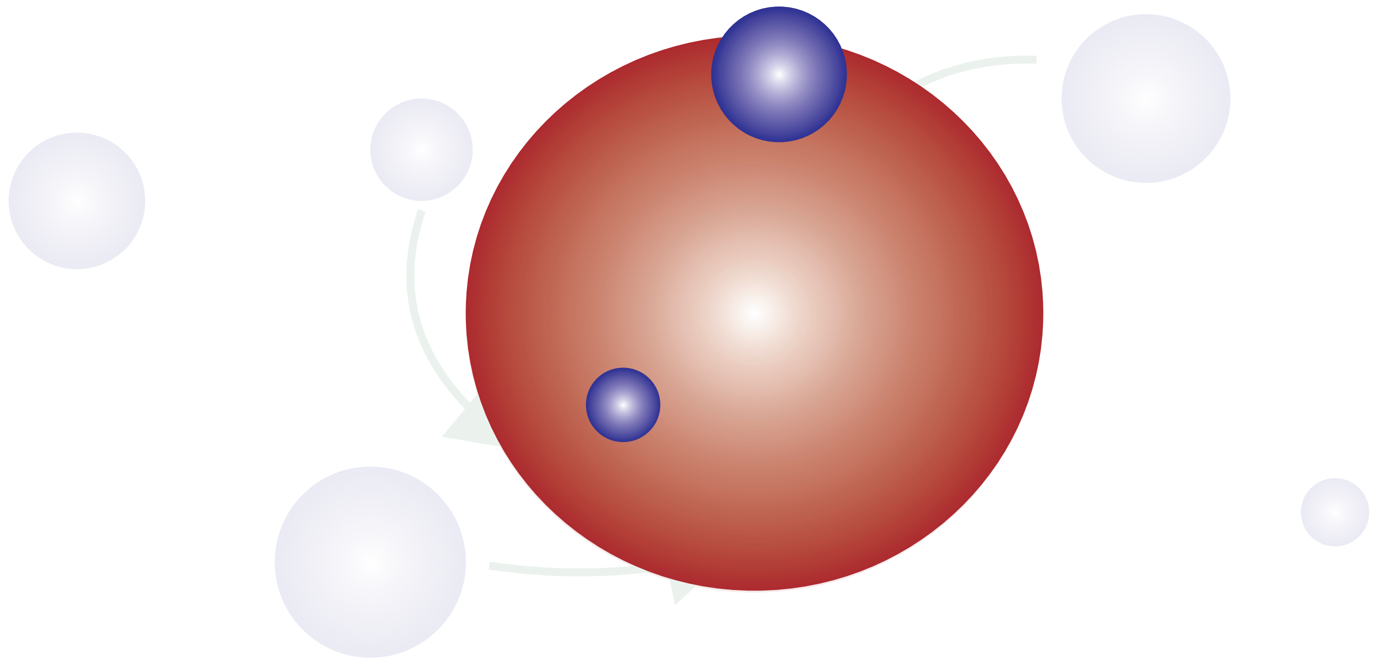

Density fluctuation

↓

Halos (including subhalos)

↓

Subhalos accrete on a host halo

↓

Satellite galaxies formed in the host halo

dSphs

Formation of dSphs

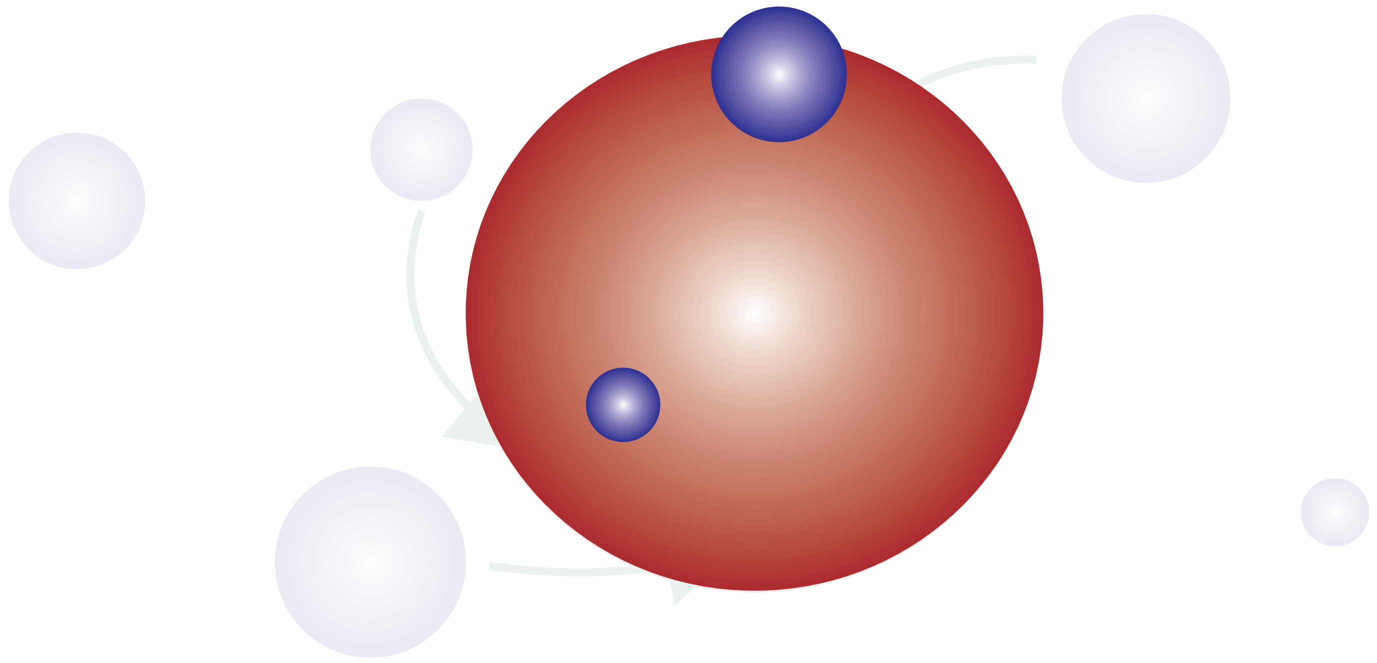

Density fluctuation

↓

Halos (including subhalos)

↓

Subhalos accrete on a host halo

↓

Satellite galaxies formed in the host halo

dSphs

Studied in semi-analytical modeling/N-body simulation

Hiroshima et al. ’18

Subhalos accrete on a host halo

↓

Satellite galaxies formed in the host halo

dSphs

Subhalos accrete on a host halo

↓ **Tidal strippling**

Satellite galaxies formed in the host halo

dSphs

Subhalos accrete on a host halo

↓ **Tidal strippling** ← Semi-analytical modeling/N-body simulation

Satellite galaxies formed in the host halo

dSphs

Hiroshima et al. '18

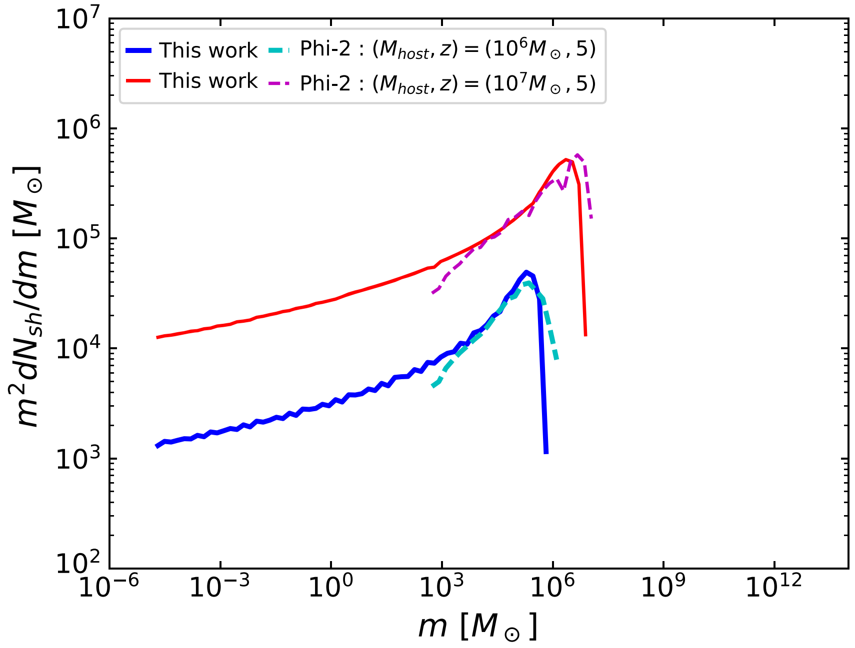

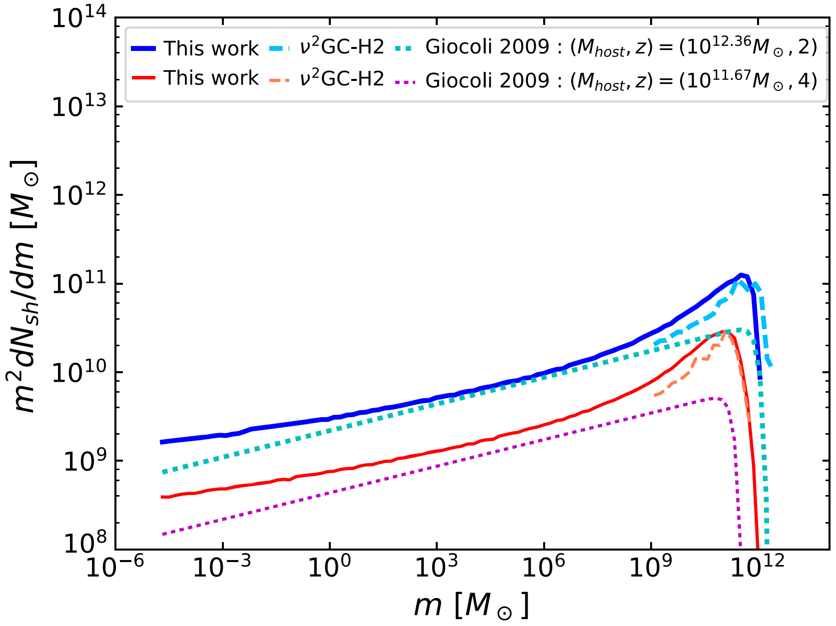

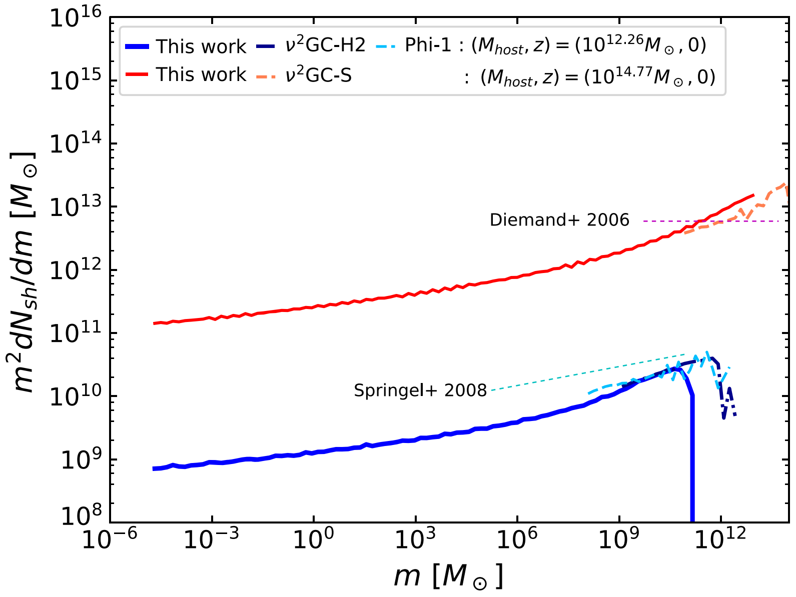

Subhalo mass distribution is given in a wide range of the mass

Subhalos accrete on a host halo

↓ **Tidal strippling**

Satellite galaxies formed in the host halo

dSphs

→ Probability distribution function (PDF) of satellites:

$$P_{\rm st} = P_{\rm sh} P_{\rm form}$$

Prior for the satellite parameters

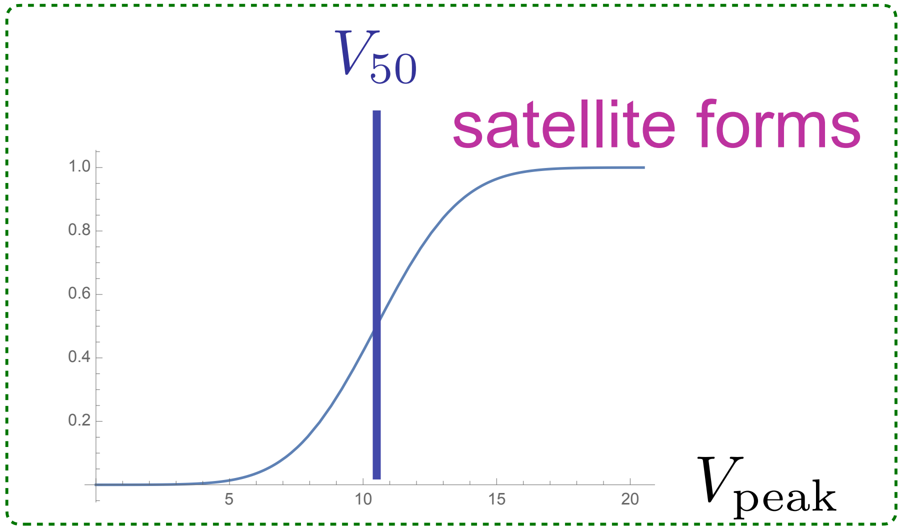

$P_{\rm sh} \propto \dfrac{d^3 N_{\rm sh}}{d\rho_s dr_s dr_t}$: PDF of subhalos

$P_{\rm form}(V_{\rm peak}; V_{50})$: probability to form a satellite galaxy from a subhalo

Subhalos accrete on a host halo

↓ **Tidal strippling**

Satellite galaxies formed in the host halo

dSphs

Satellite galaxy
≈
dSph

→ Probability distribution function (PDF) of satellites:

$$P_{\rm st} = P_{\rm sh} P_{\rm form}$$

Prior for the satellite parameters

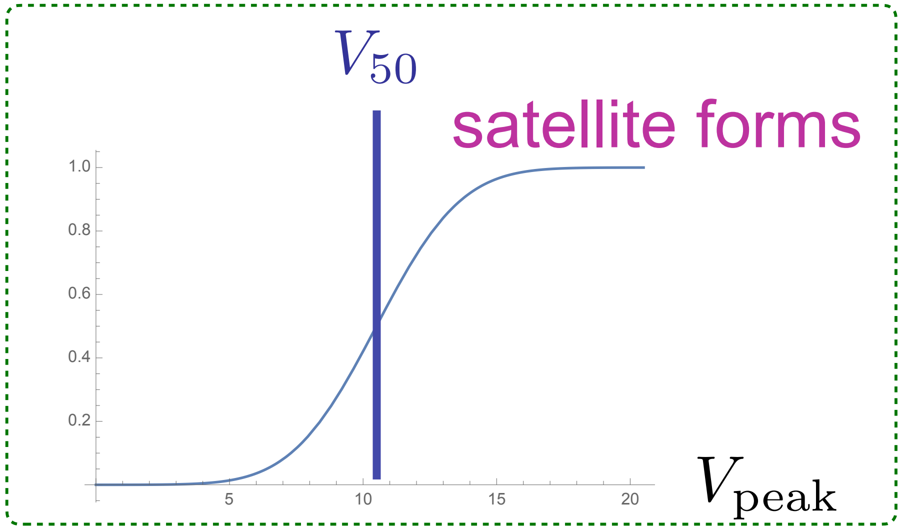

$P_{\rm sh} \propto \dfrac{d^3 N_{\rm sh}}{d\rho_s dr_s dr_t}$: PDF of subhalos

$P_{\rm form}(V_{\rm peak}; V_{50})$: probability to form a satellite galaxy from a subhalo

Now we have

- *Prior* PDF for satellite parameters (ρ_s, r_s, r_t)

→

$$P_{\rm st} \propto \frac{d^3 N_{\rm sh}}{d\rho_s dr_s dr_t} P_{\rm form}$$

- Likelihood function of obtaining $(\theta_h, \sigma_{\rm los}, D)$ for each dSph

→

$$\mathcal{L}_{\rm data} = \prod_{x=\{\theta_h, \sigma_{\rm los}, D\}} \frac{1}{\sqrt{2\pi\sigma_x^2}} \exp\left[-\frac{(x - x_{\rm obs})^2}{2\sigma_x^2}\right]$$

Now we have

- *Prior* PDF for satellite parameters (ρ_s, r_s, r_t)

$$\longrightarrow \qquad P_{\rm st} \propto \frac{d^3 N_{\rm sh}}{d\rho_s dr_s dr_t} P_{\rm form}$$

- Likelihood function of obtaining $(\theta_h, \sigma_{\rm los}, D)$ for each dSph

$$\longrightarrow \quad \mathcal{L}_{\rm data} = \prod_{x=\{\theta_h, \sigma_{\rm los}, D\}} \frac{1}{\sqrt{2\pi\sigma_x^2}} \exp\left[-\frac{(x - x_{\rm obs})^2}{2\sigma_x^2}\right]$$

$$\Big\downarrow$$

Bayes' Theorem

Posterior PDF for satellite parameters

$$P(\{\rho_s, r_s, r_t\}|{\rm data}) \propto \mathcal{L}_{\rm data} P_{\rm st}$$

Excluded by Geringer-Sameth et al. ’15
“GS15 cut”

Ando et al. ’20

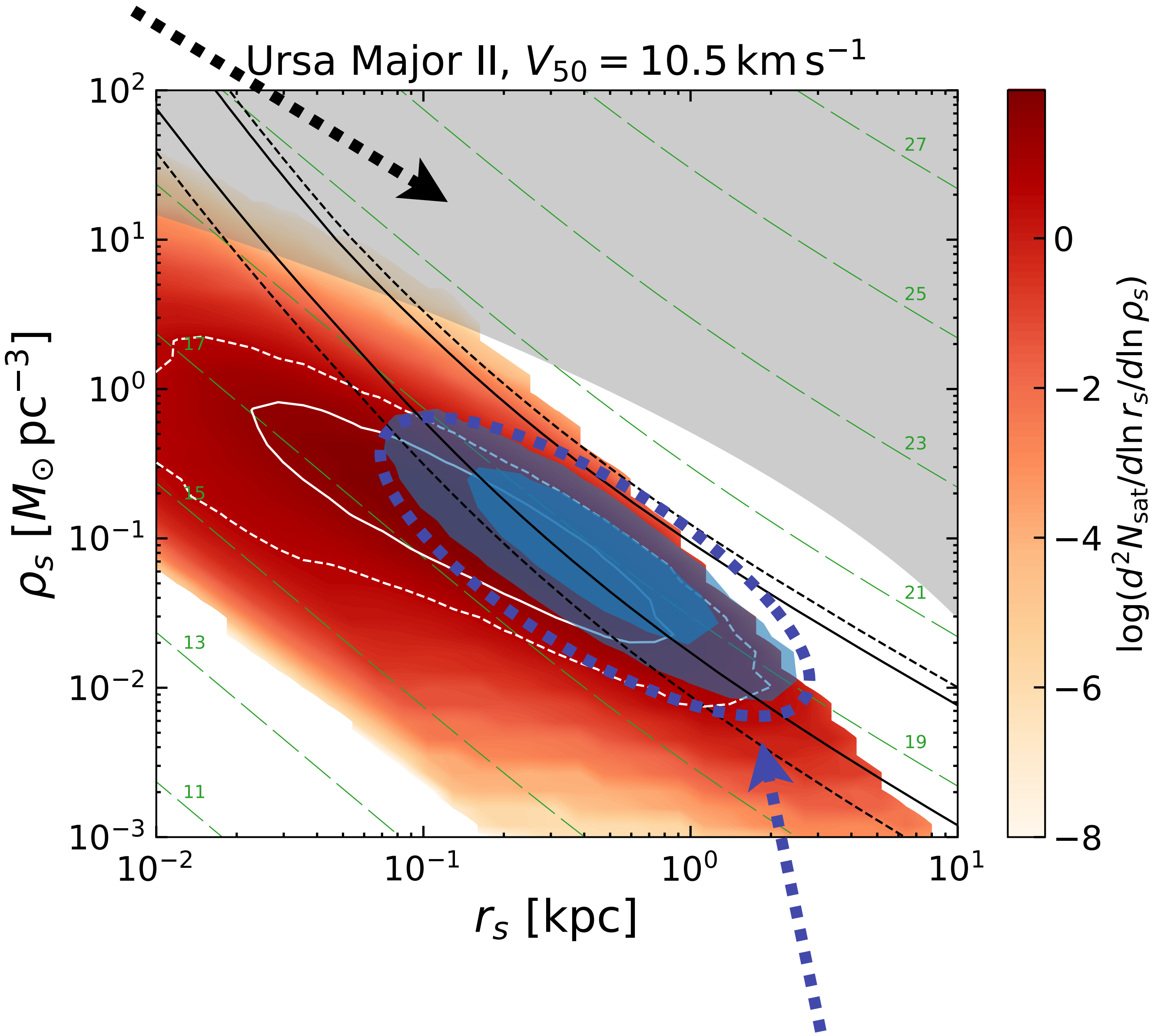

$$P(\{\rho_s, r_s, r_t\}|\mathrm{data})$$

Satellite (dSph) parameters are determined more accurately

Excluded by
“GS15 cut”

Geringer-Sameth et al. ’15

Ando et al. ’20

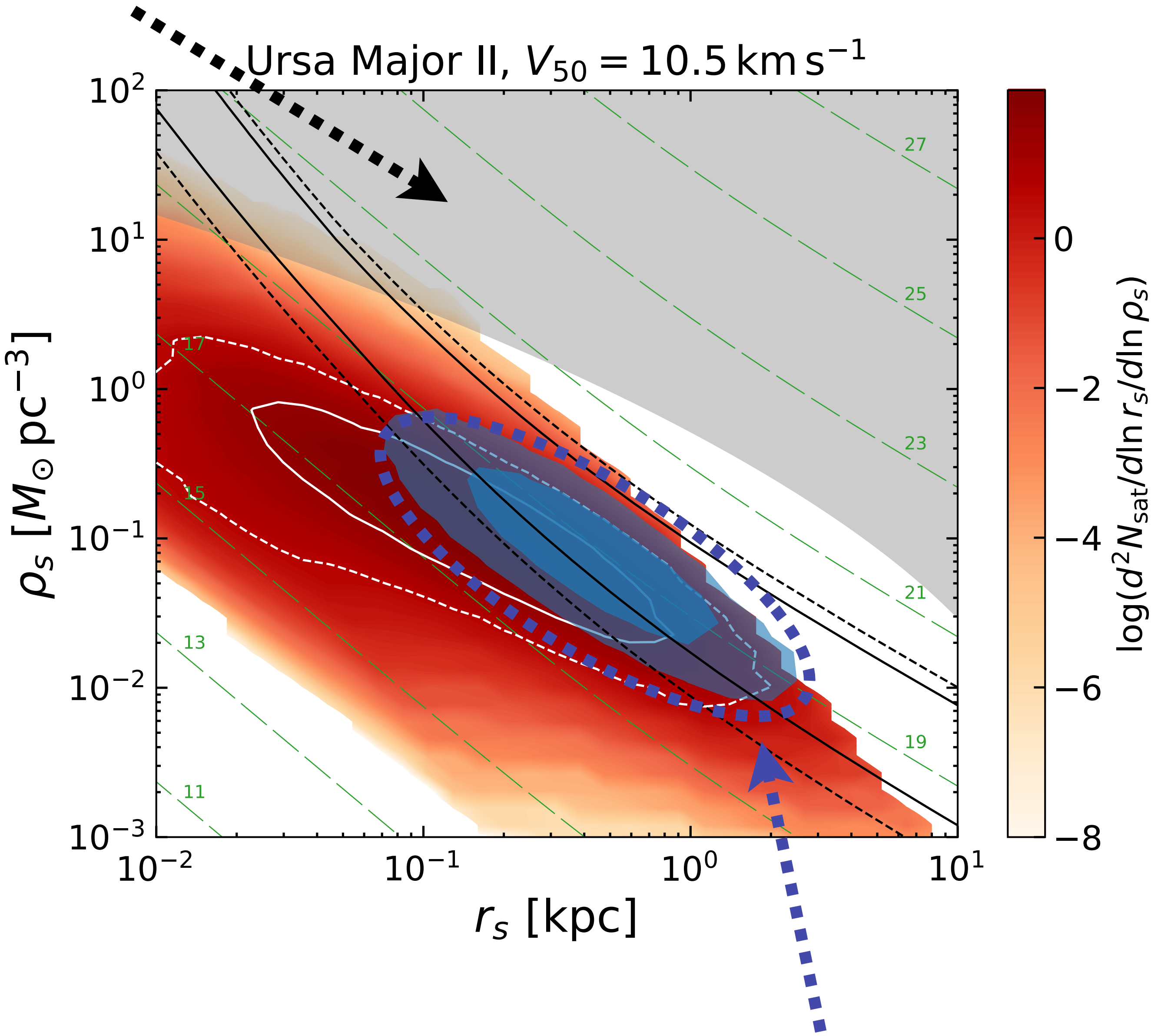

$$P(\{\rho_s, r_s, r_t\}|\mathrm{data})$$

Satellite (dSph) parameters are determined more accurately

→ We can apply it to the detection of Wino DM

Gamma-ray flux from dSphs

$$\frac{d\Phi_\gamma}{dE} = \boxed{J(\theta)} \boxed{\frac{\sigma v}{8\pi m_{\mathrm{dm}}^2} \frac{dN_\gamma}{dE}}$$

J-factor
(depending on dSphs)

DM model

Gamma-ray flux from dSphs

$$\frac{d\Phi_\gamma}{dE} = J(\theta)\frac{\sigma v}{8\pi m_{\rm dm}^2}\frac{dN_\gamma}{dE}$$

J factor
(depending on dSphs)

Wino DM model

Gamma-ray from Wino annihilation

$$\frac{\sigma v}{8\pi m_{\rm dm}^2}\frac{dN_\gamma}{dE}$$

Gamma-ray from Wino annihilation

$$\frac{\sigma v}{8\pi m_{\rm dm}^2}\frac{dN_\gamma}{dE} = \frac{1}{8\pi \underbrace{\boxed{m_{\rm dm}^2}}_{\text{Wino mass}}}\sum_i \overbrace{\boxed{\sigma v_i \left[\frac{dN_\gamma}{dE}\right]_i}}^{\text{Annihilation cross section and gamma-ray spectrum}}$$

$$i = \gamma\gamma,\ \gamma Z,\ ZZ\,, W^+W^-$$

Gamma-ray from Wino annihilation

Sommerfeld enhancement

Annihilation cross section
and gamma-ray spectrum

$$\frac{\sigma v}{8\pi m_{\rm dm}^2}\frac{dN_\gamma}{dE} = \frac{1}{8\pi \boxed{m_{\rm dm}^2}}\sum_i \boxed{\sigma v_i \left[\frac{dN_\gamma}{dE}\right]_i}$$

Wino mass

$$i = \gamma\gamma,\ \gamma Z,\ ZZ\,, W^+W^-$$

Sommerfeld effect

e.g., attractive Yukawa potential (light scalar mediator)

m_ϕ : mediator mass

$$\epsilon_\phi = \frac{m_\phi}{\alpha_y m_{\rm dm}}$$

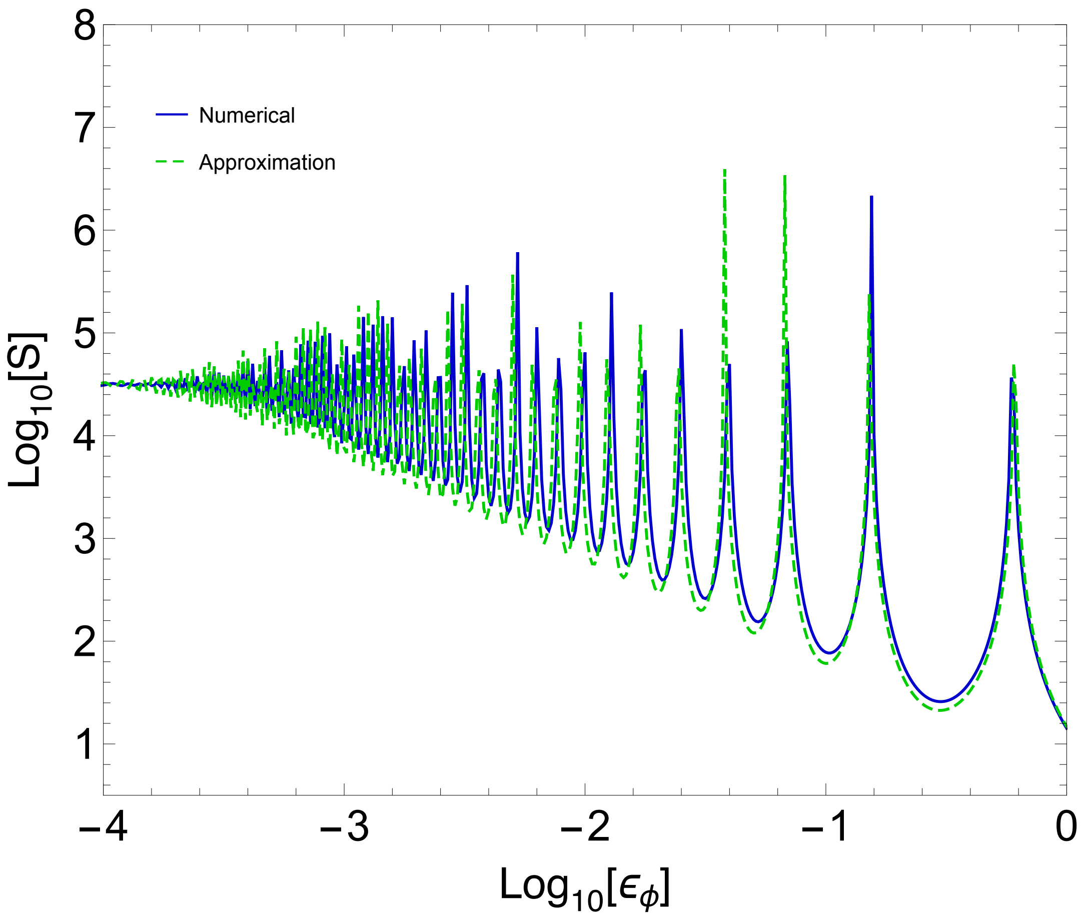

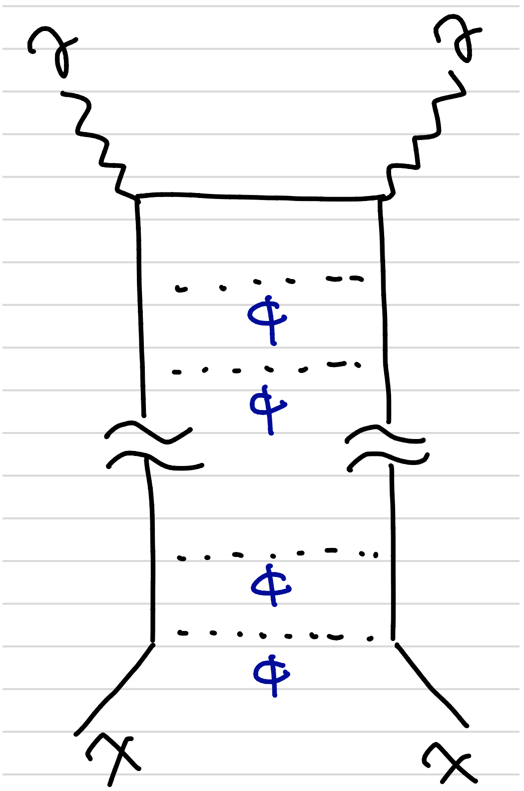

Large enhancement in the cross section

Sommerfeld enhanced Wino annihilation cross section

Hisano et al. ’05

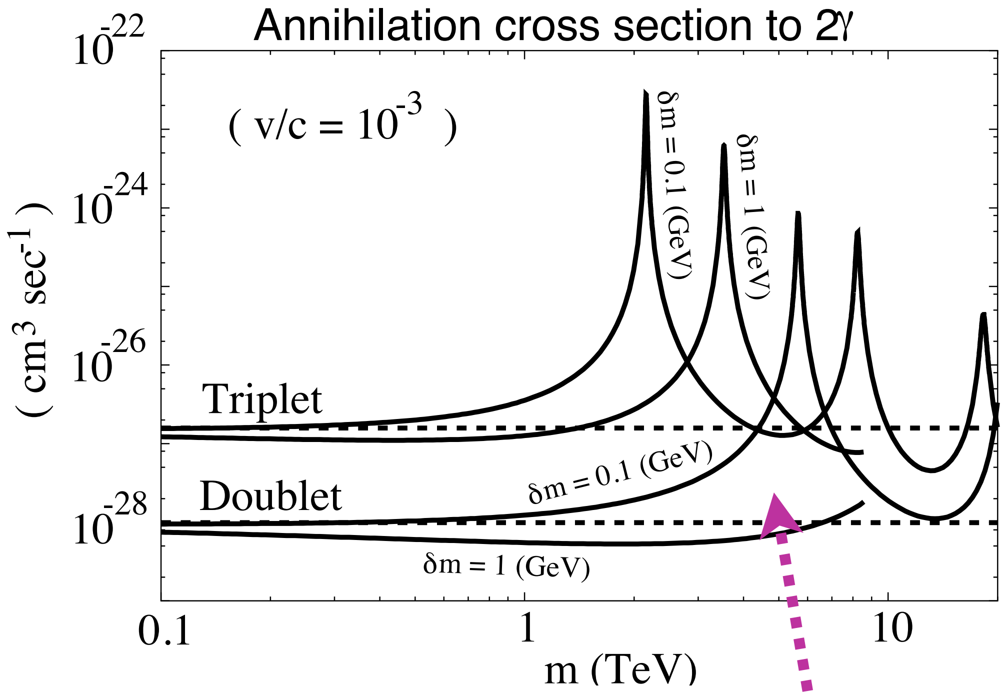

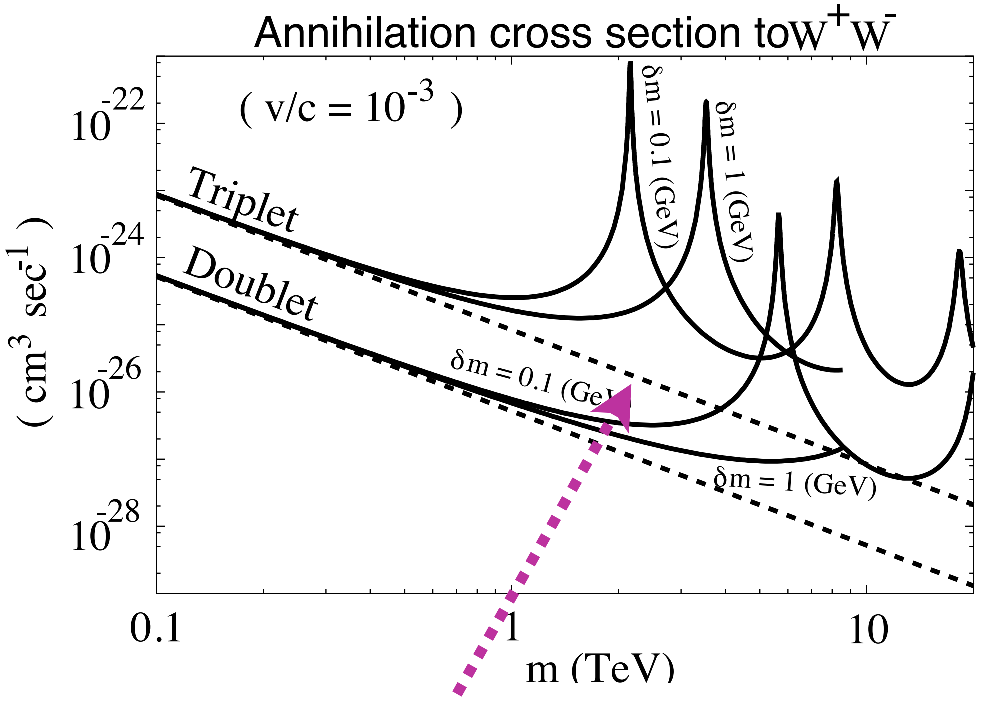

Enhancement at a certain mass

Sommerfeld enhanced Wino annihilation cross section

(at the next-to-leading log level)

Baumgart et al. ’18, ’19
Beneke et al. ’20, ’21

Additional corrections to γ-flux

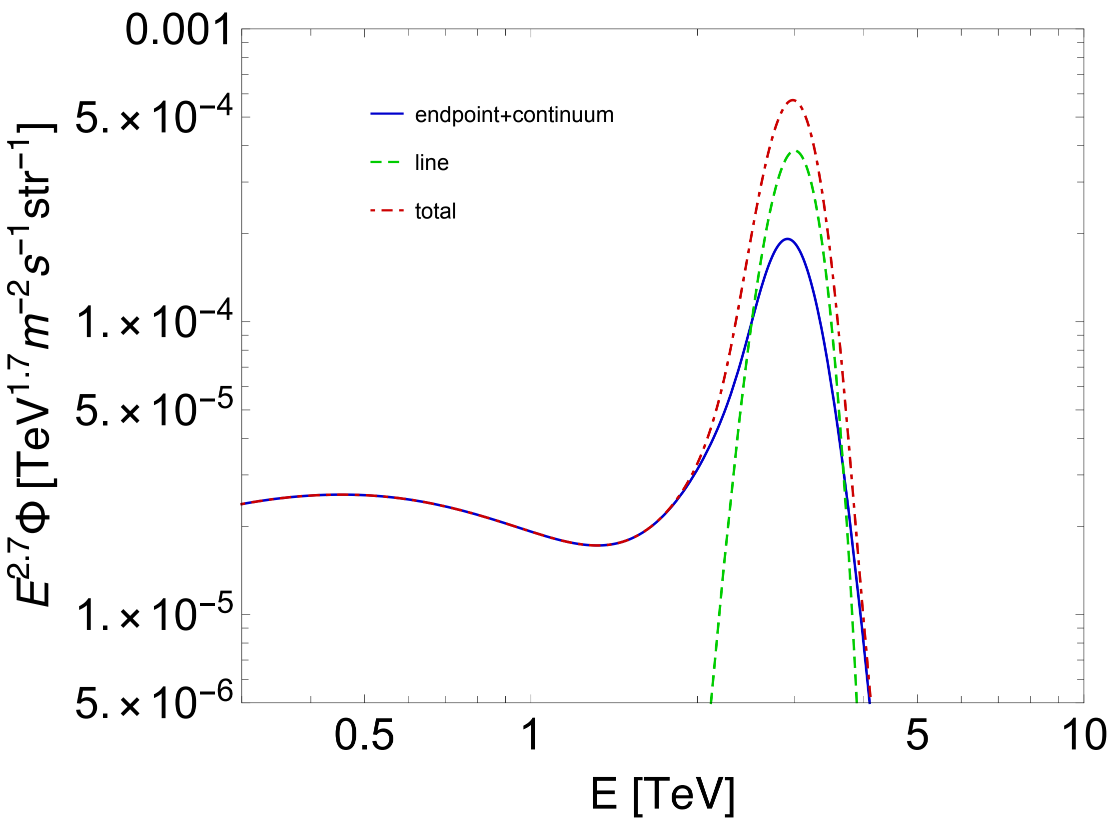

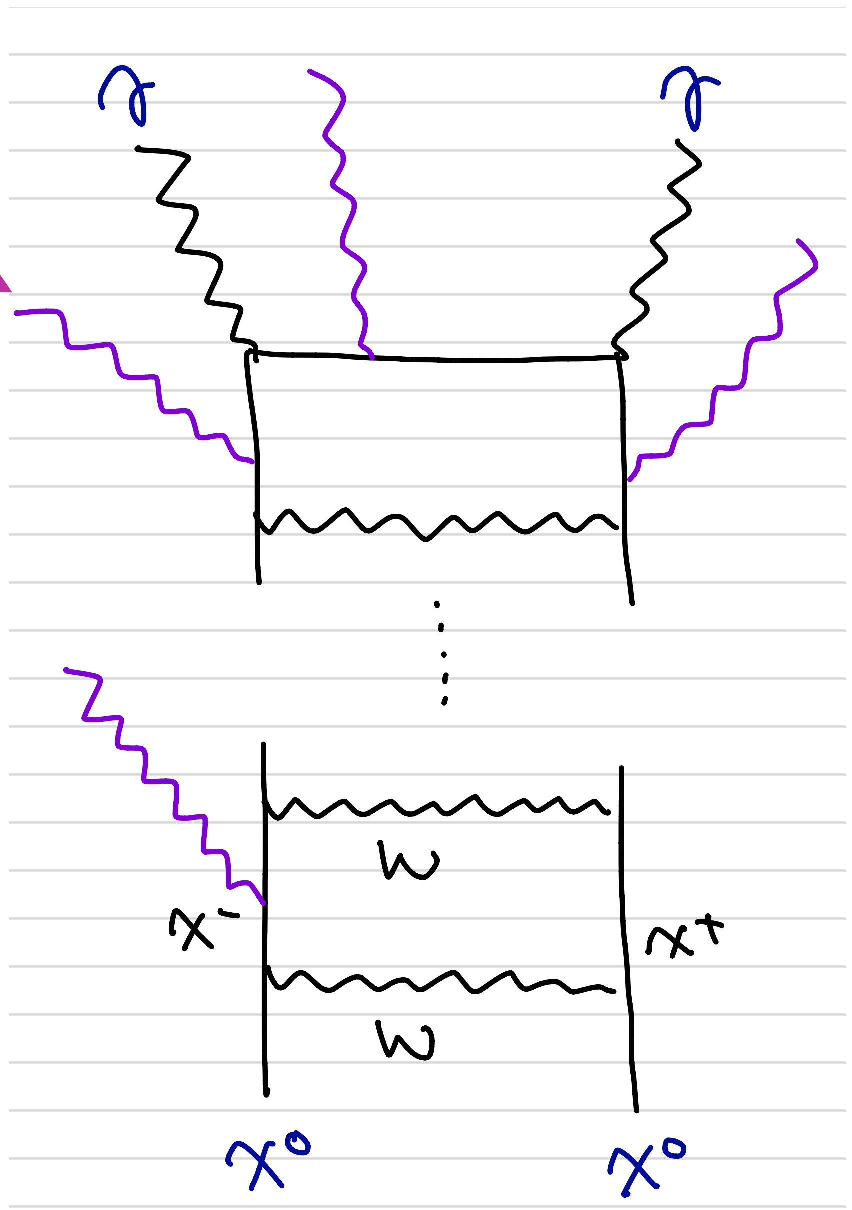

3. Numerical results

dSph: Ursa Major II

Ando, KI ’21

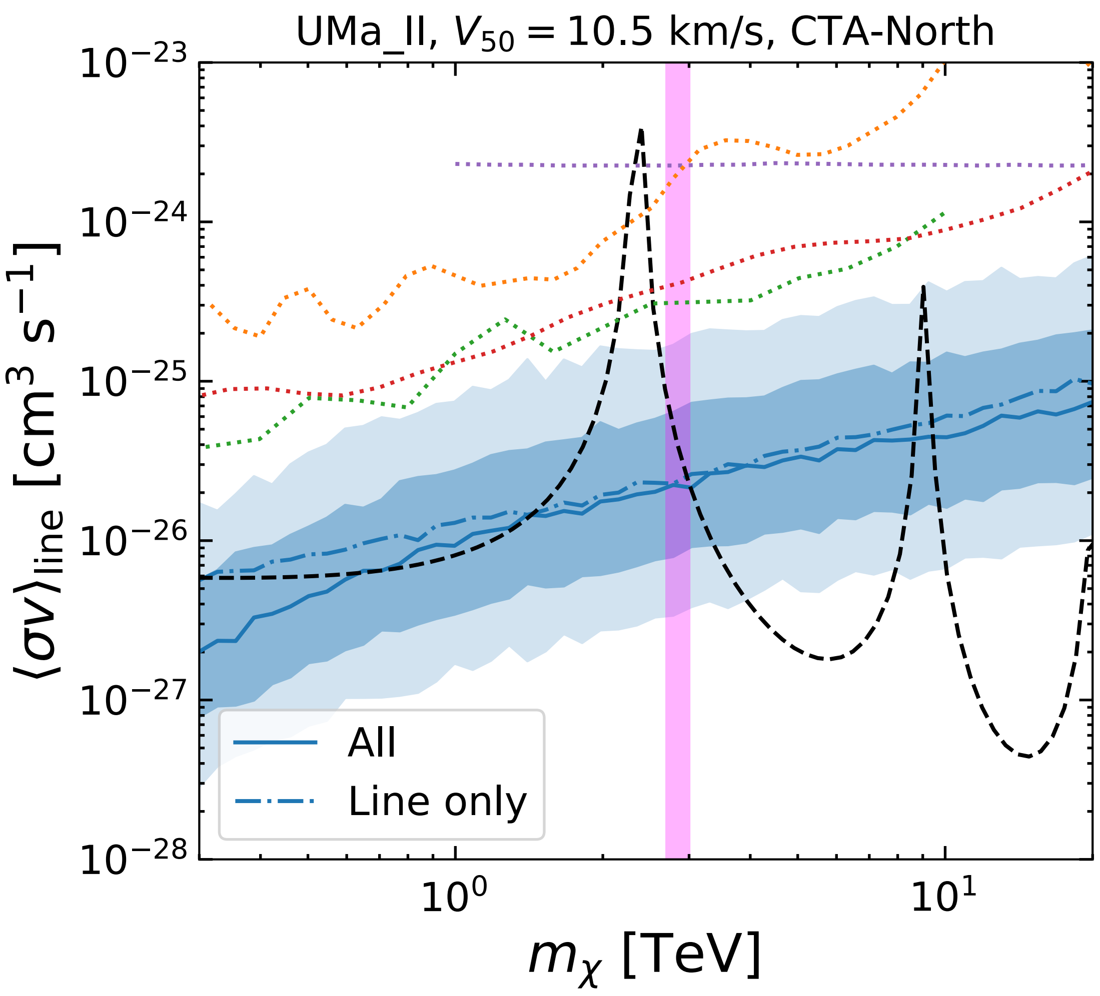

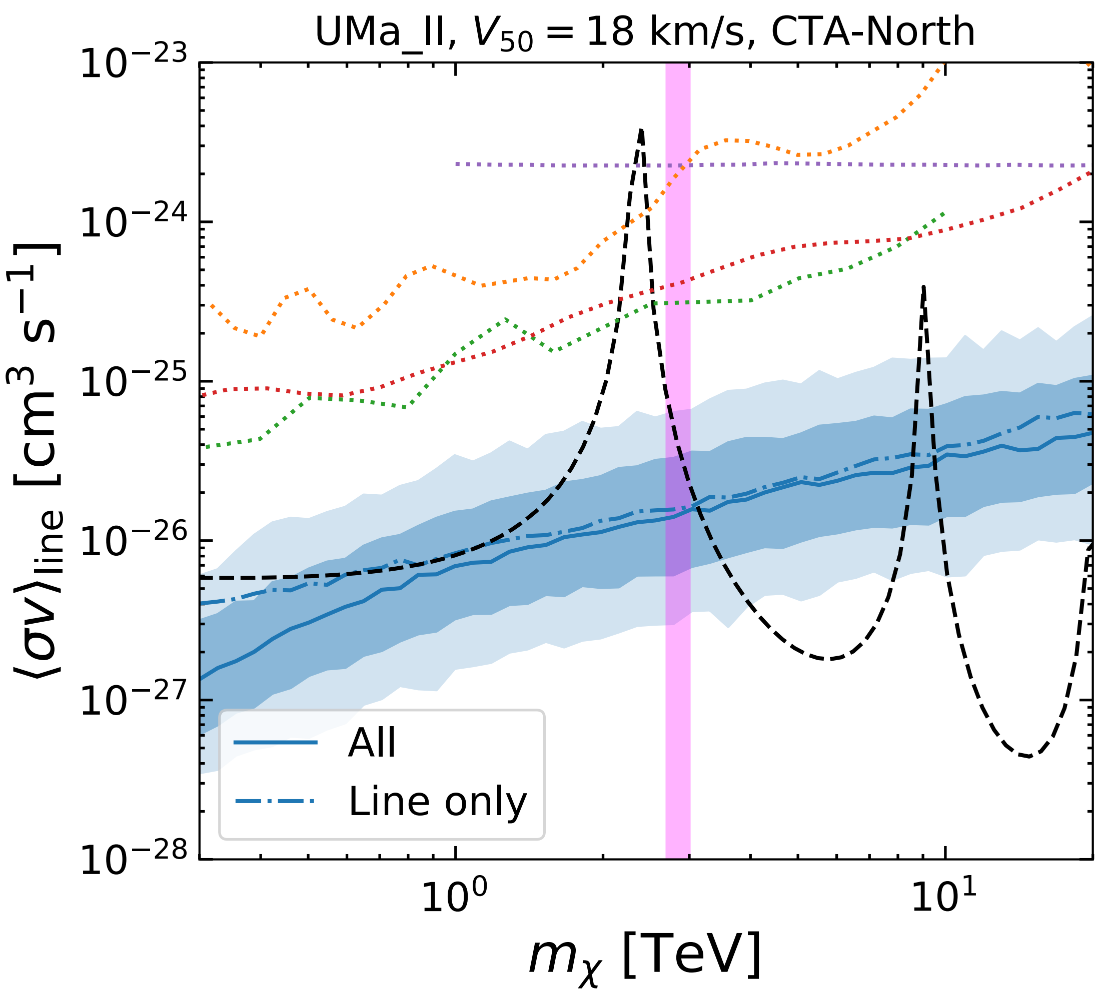

dSph: Ursa Major II

Ando, KI '21

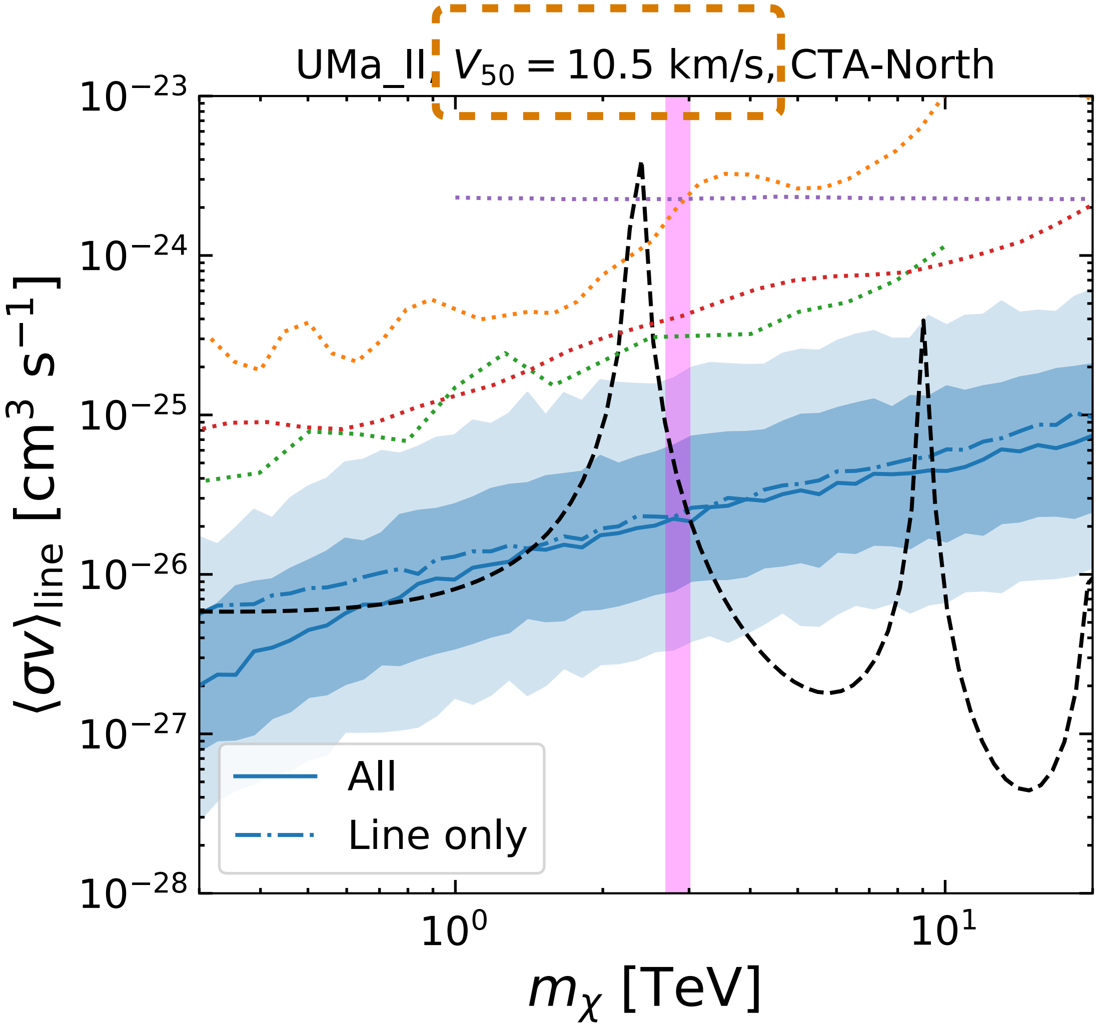

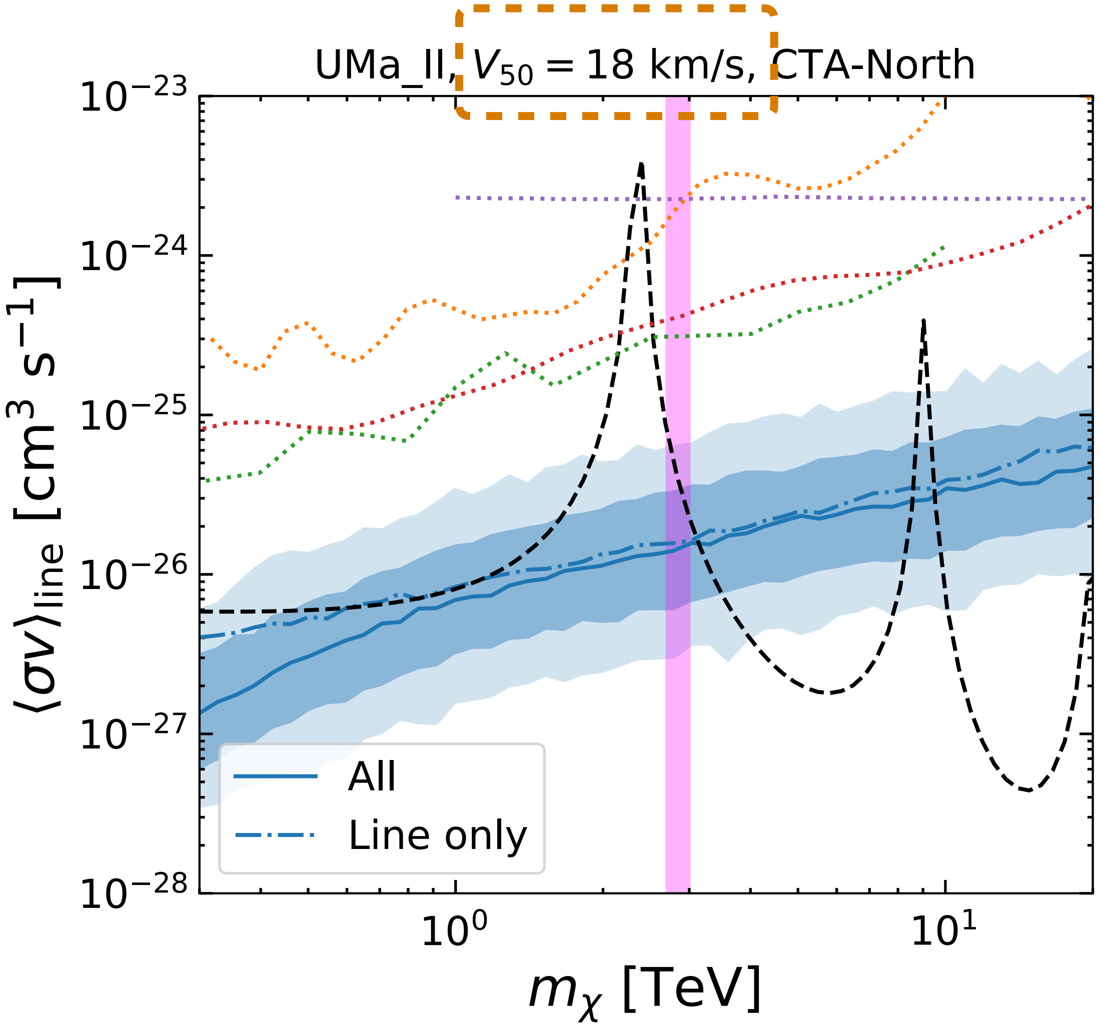

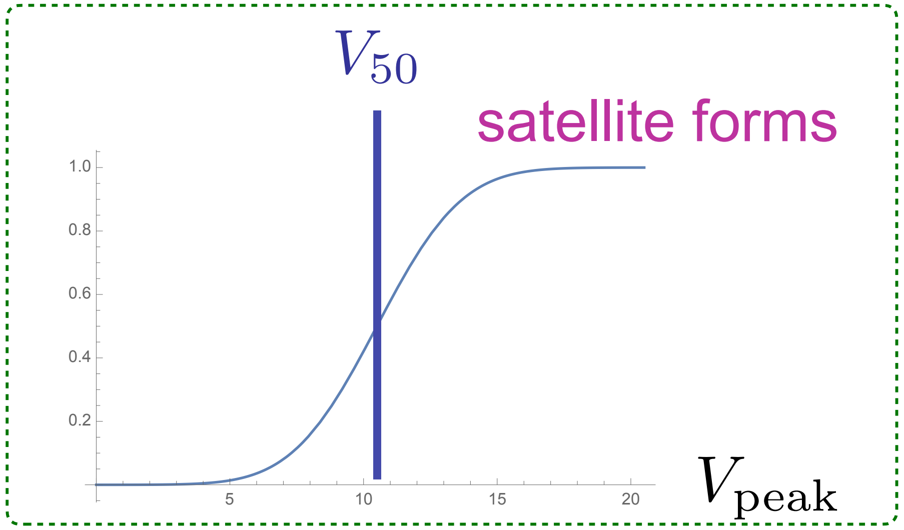

dSph: Ursa Major II

Ando, KI '21

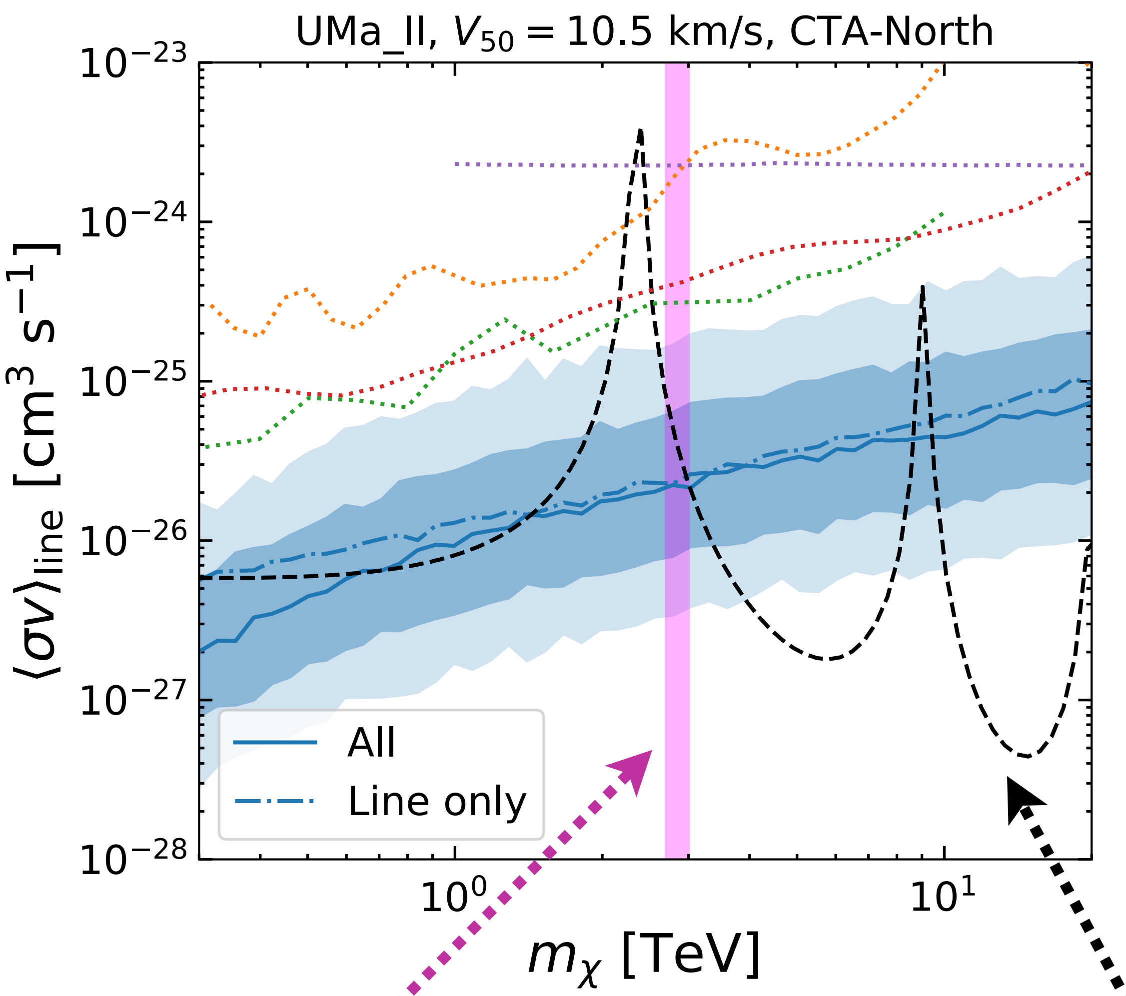

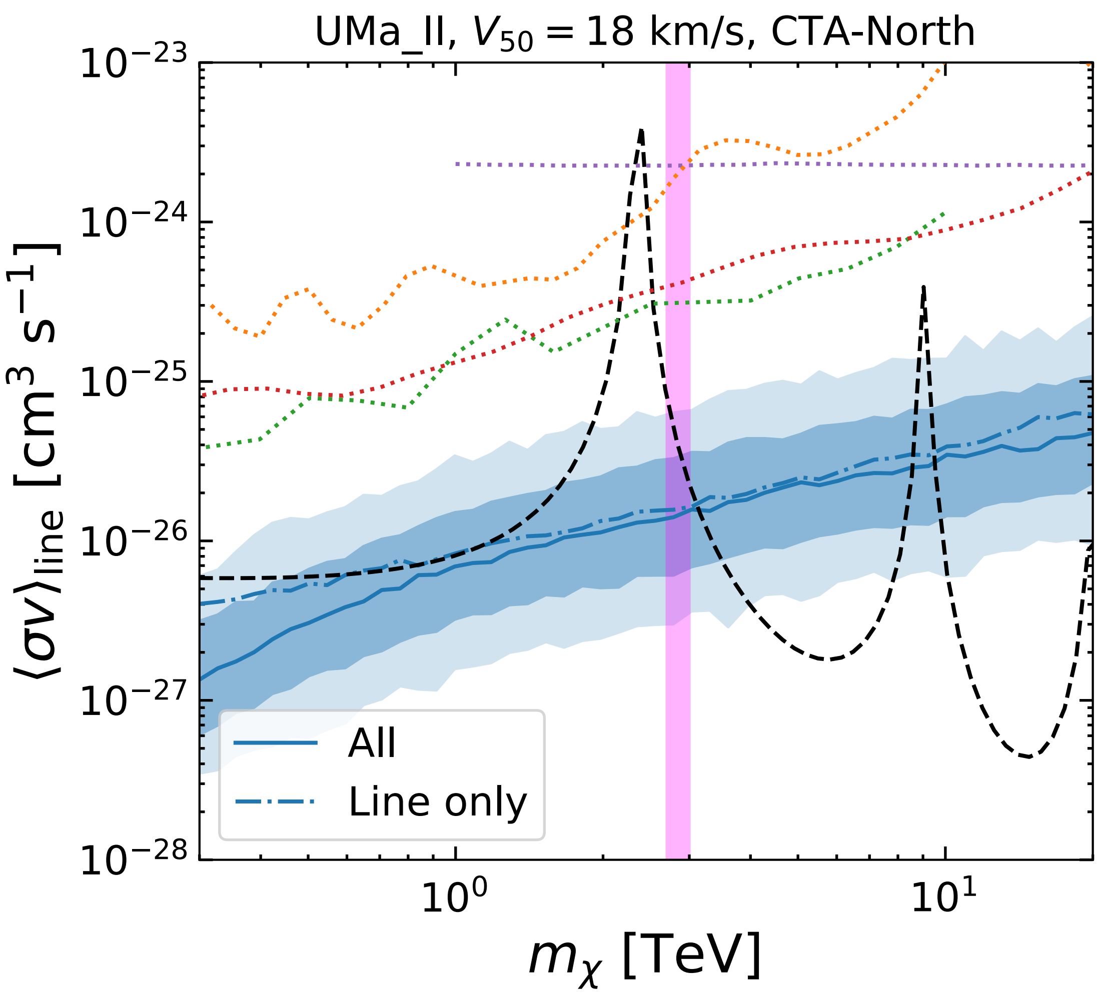

Thermal Wino DM range
$(2.7 - 3\,\mathrm{TeV})$

$$\sigma v_{\rm line} \equiv \sigma v_{\gamma\gamma} + \frac{1}{2}\sigma v_{\gamma Z}$$

dSph: Ursa Major II

The current constraints

Ando, KI '21

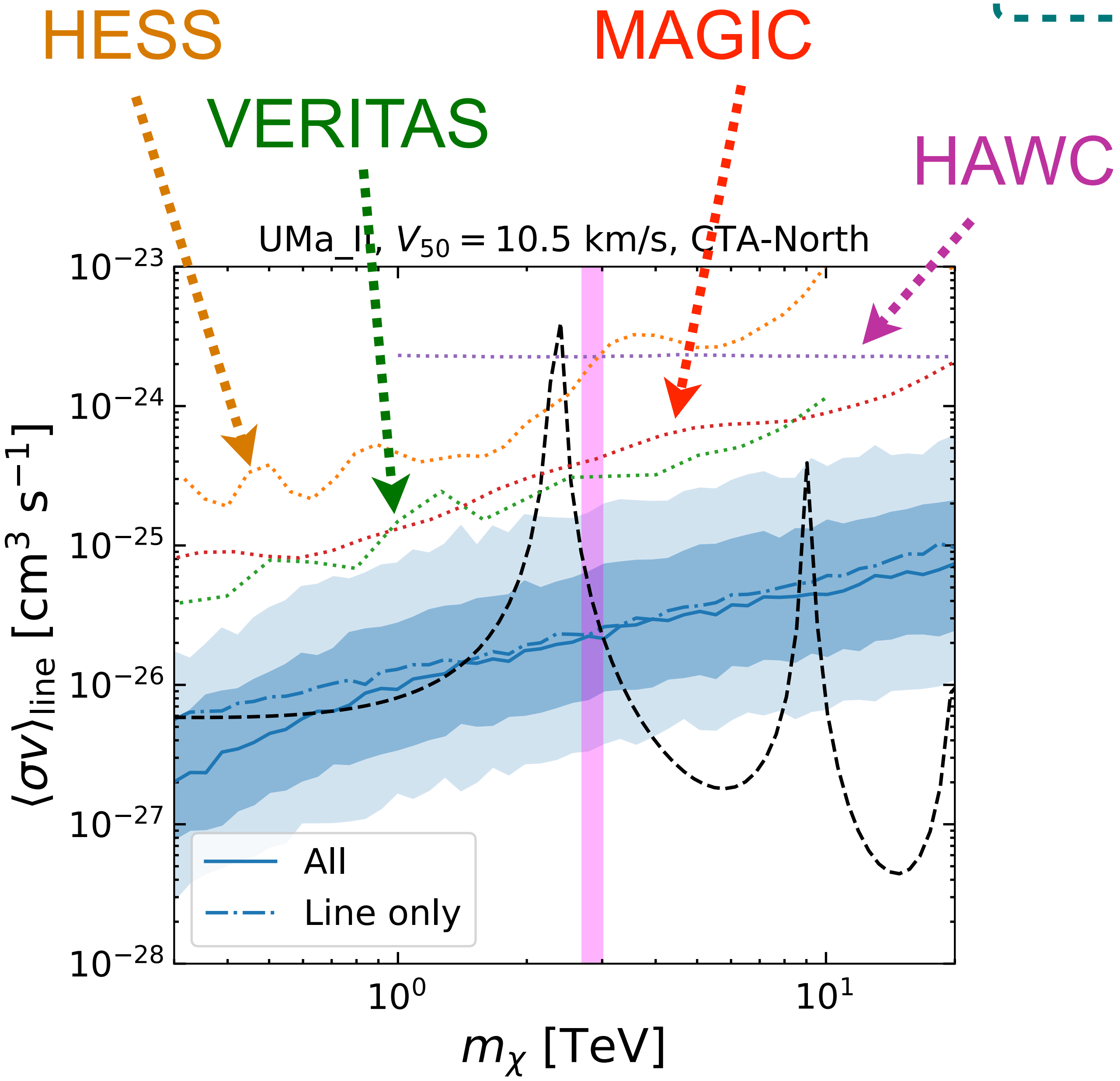

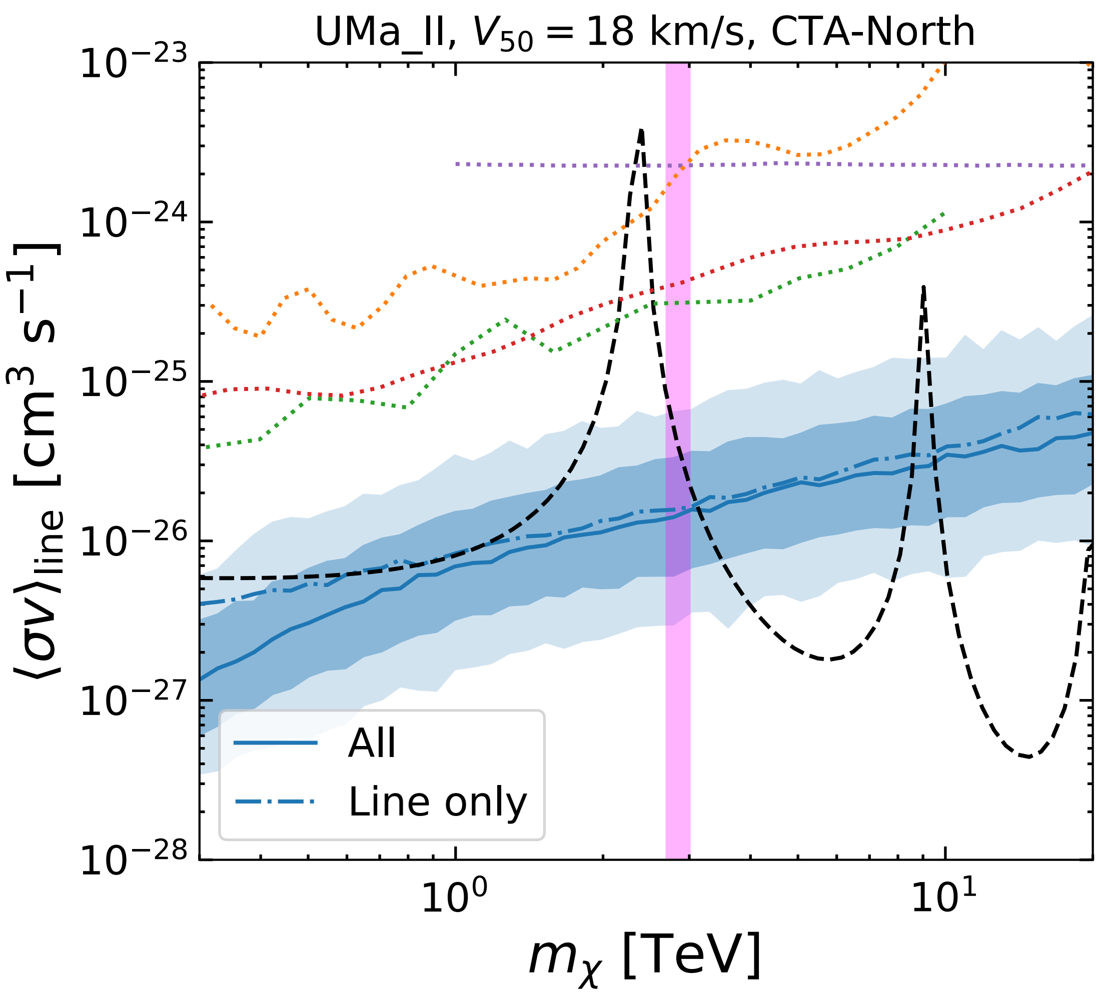

dSph: Ursa Major II

CTA sensitivity (500h)

Ando, KI ’21

Expected 95% upper limit

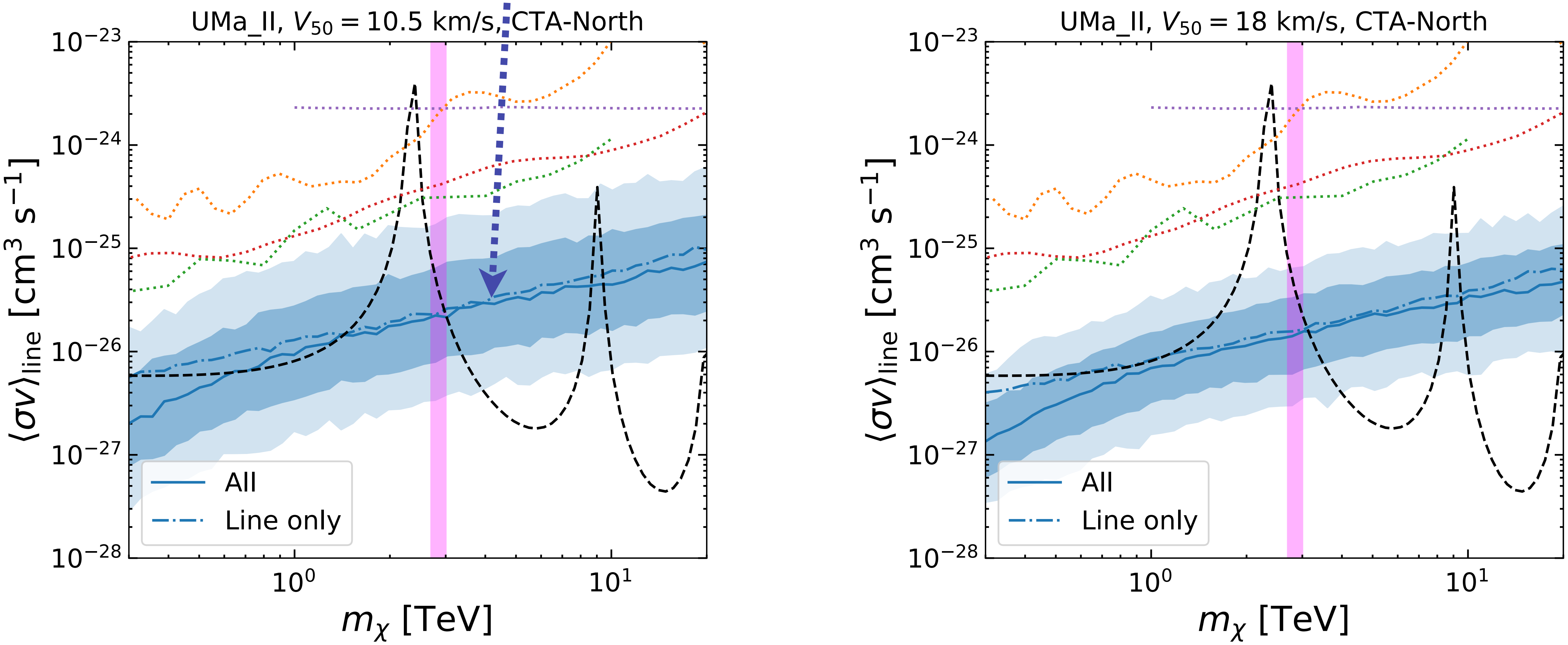

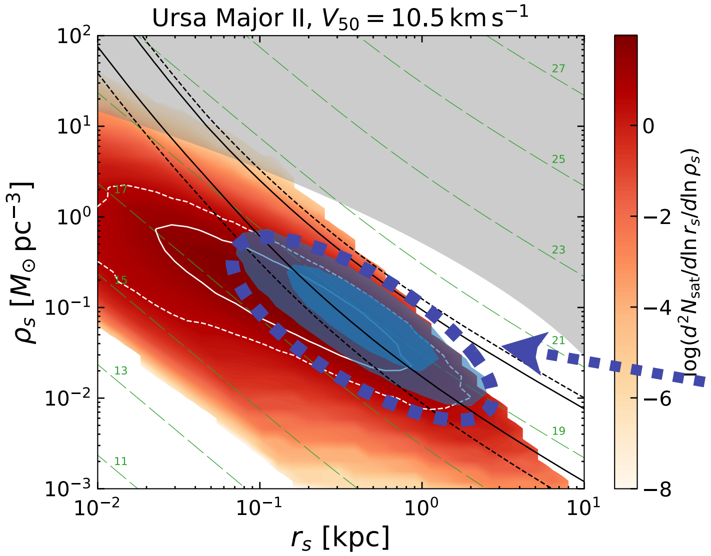

Band correspond to 68% (95%) range for the limit, which comes from the estimation of J-factor

dSph: Ursa Major II

CTA sensitivity (500h)

Ando, KI ’21

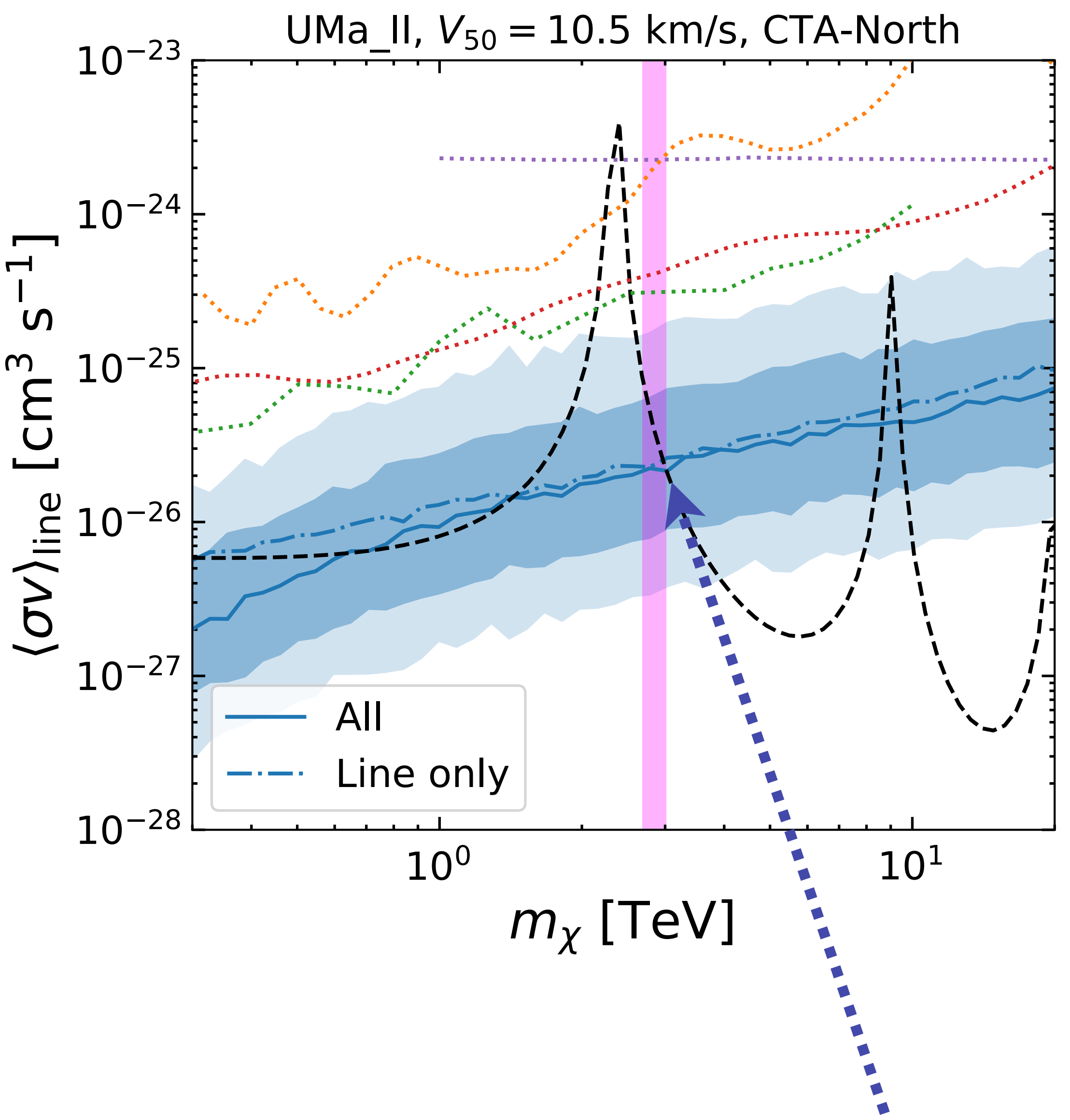

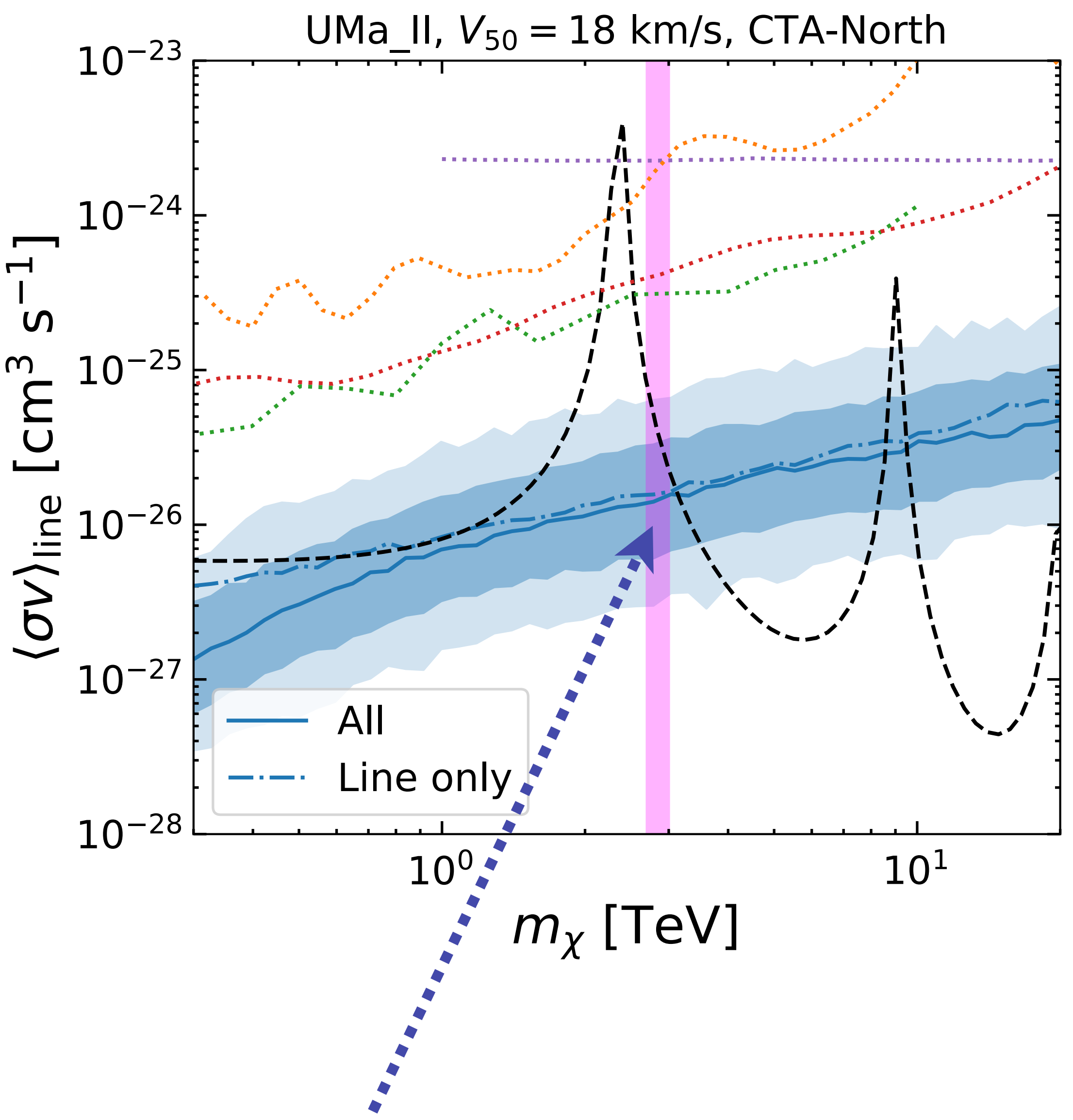

Thermal Wino DM can be detected by CTA observation

Other possible targets

Ando, KI ’21

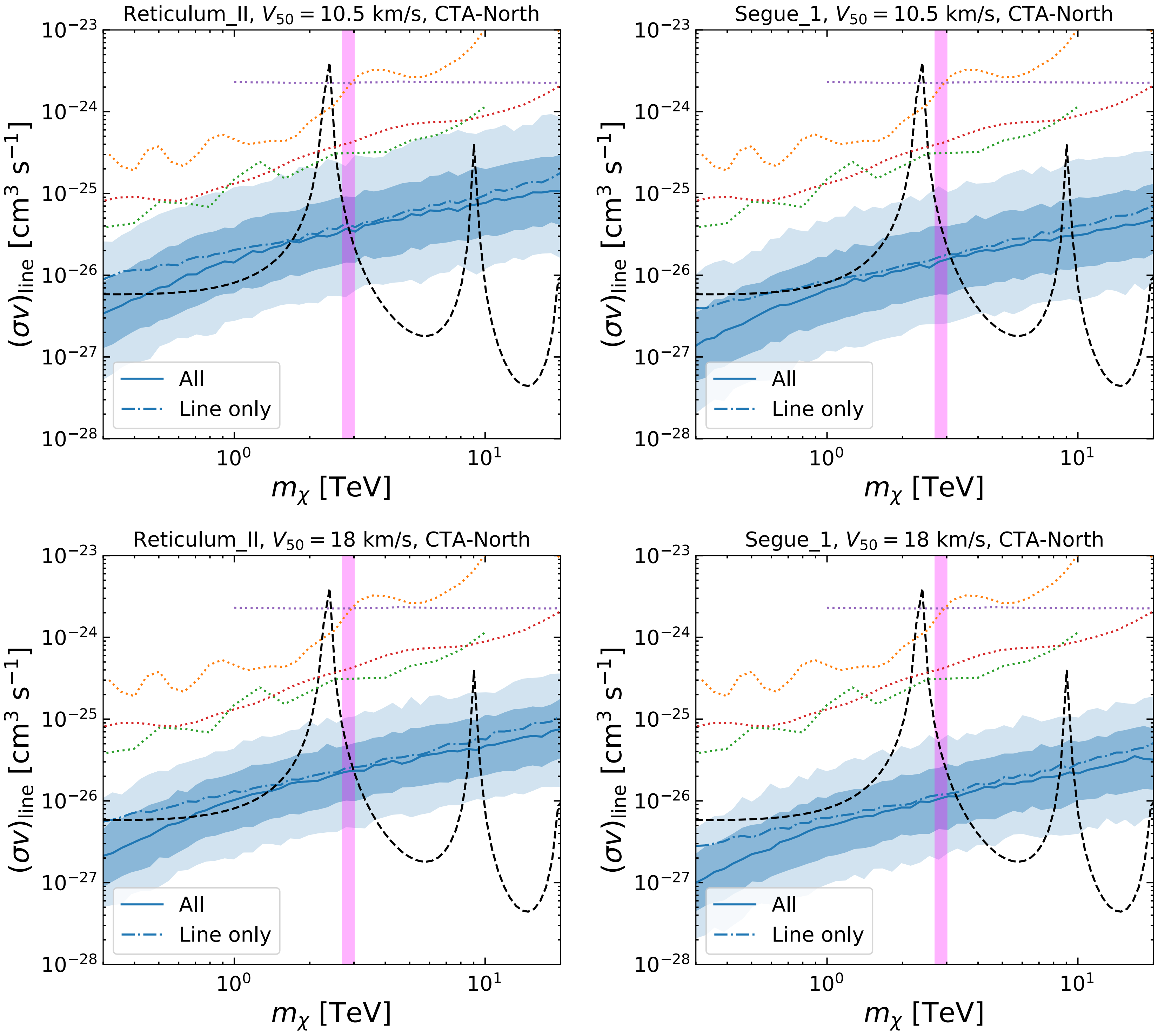

Reticulum II and Segue 1 are also good candidates to detect thermal Wino DM

4. Conclusions

We have studied γ-ray signals from the Wino DM in dSphs

- J-factor is determined by the prior distributions for satellite parameters that are given by semi-analytic modeling/N-body simulations
- Thermal Wino DM can be detected in CTA observation

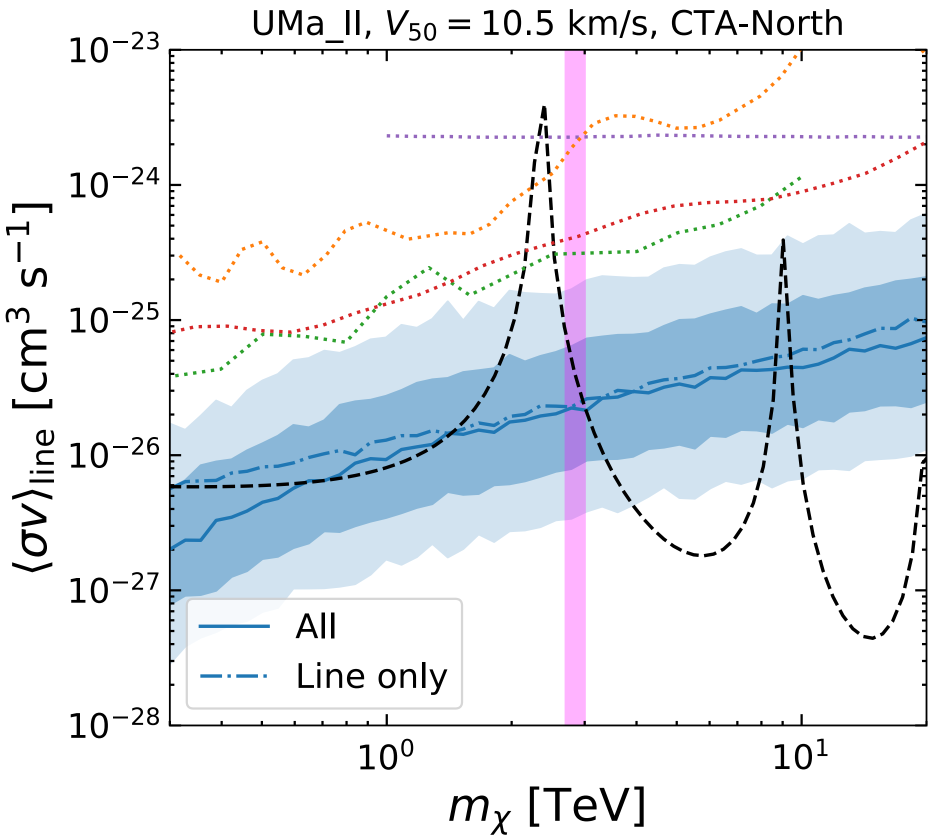

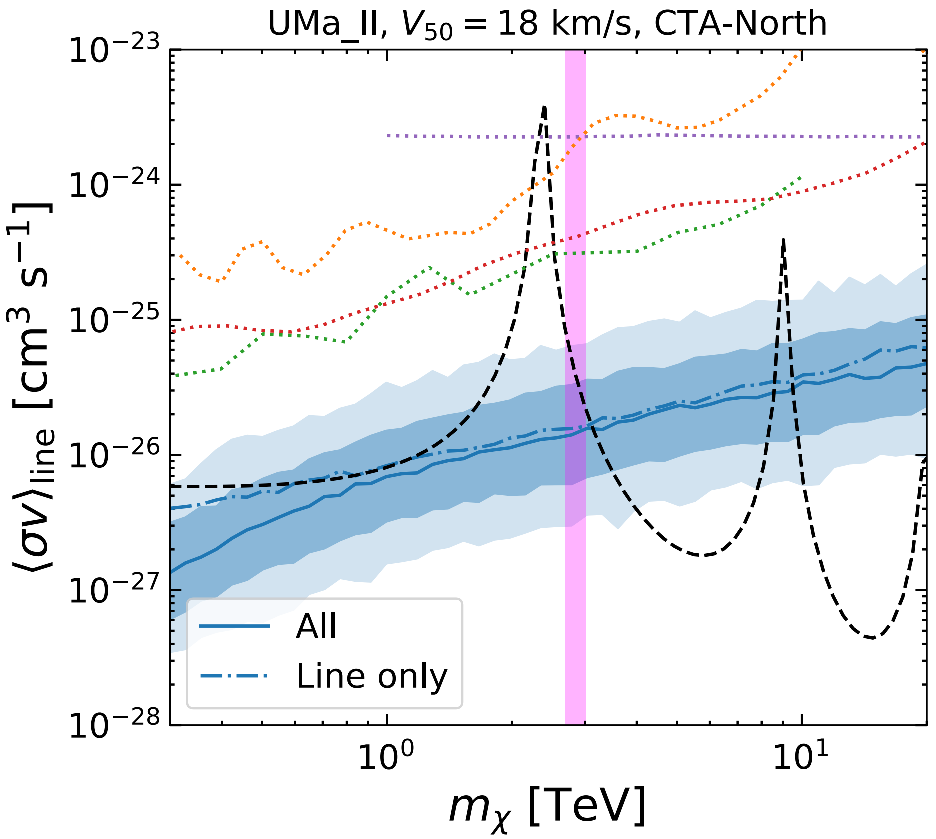

Backups

J-factor in a light mediator model

Ando, KI '21

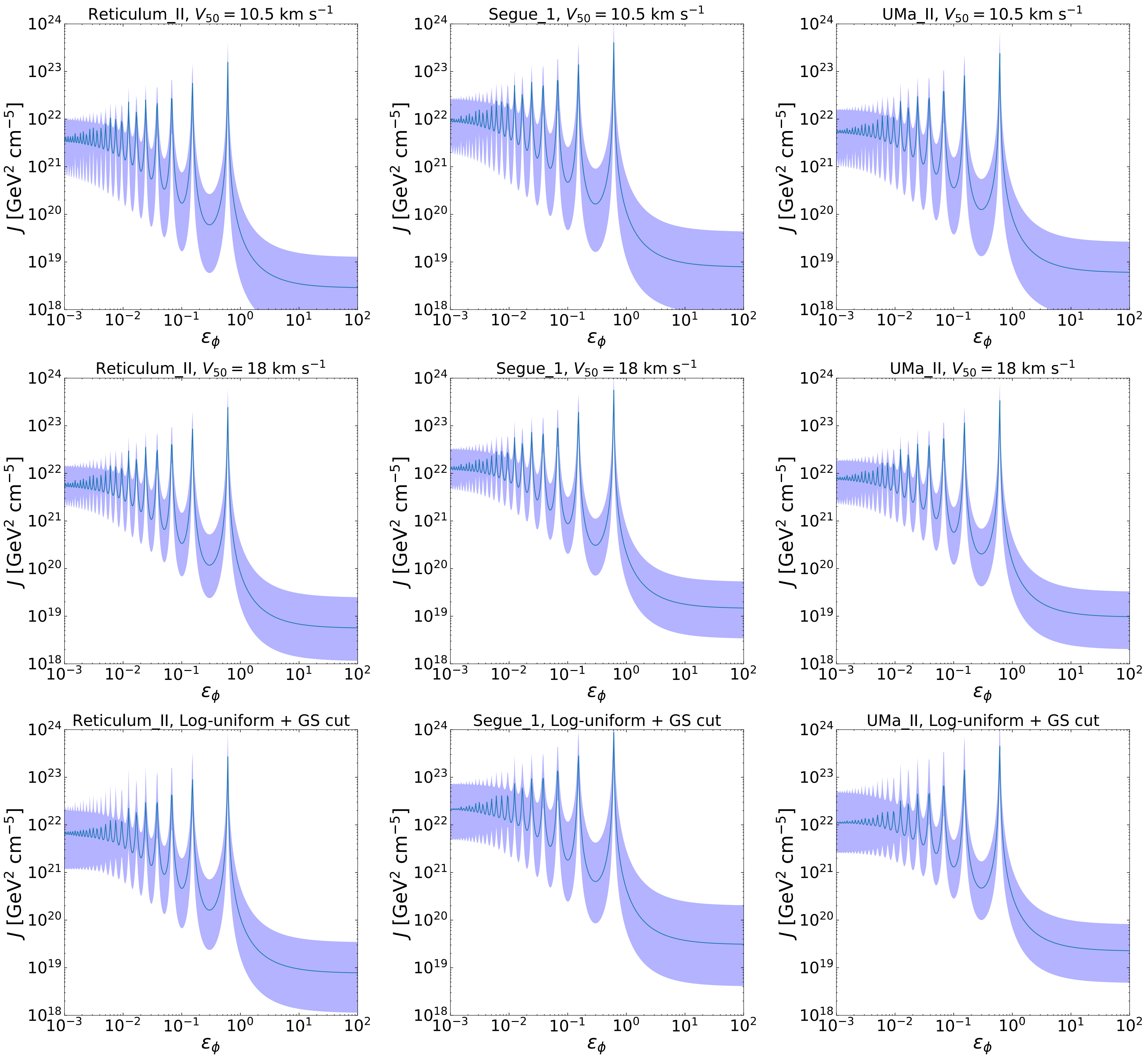

Annihilation cross section in a light mediator model

Ando, KI '21